

https://dspace.org/

The influence of El Niño Southern Oscillation (ENSO) on rainfall over the mega-dam region of South Africa

Abubakar, Mohamed

2025-08

University of the Witwatersrand, Johannesburg

https://hdl.handle.net/10539/50122

Abubakar, Mohamed. (2025). The influence of El Niño Southern Oscillation (ENSO) on rainfall over the mega-dam region of South Africa. [Master's dissertation, University of the Witwatersrand, Johannesburg]. WIReDSpace. https://hdl.handle.net/10539/50122

Downloaded from a DSpace repository. https://dspace.org/



UNIVERSITY OF THE
WITWATERSRAND,
JOHANNESBURG

The influence of El Niño Southern Oscillation (ENSO) on rainfall over the mega-dam region of South Africa

Mohamed Abubakar (1392355)

School of Geography, Archaeology and Environmental Studies

University of the Witwatersrand

Supervisors: Dr Jessica Steinkopf and Prof Francois Engelbrecht

August 2025

Declaration

I hereby declare that this dissertation is my own, unaided work. It is being submitted for the degree of Master of Science (MSc) at the University of the Witwatersrand, Johannesburg. It has not been submitted before for any degree or examination at any other university.

Mohamed Abubakar

26/08/2025

Acknowledgements

I would like to express my deepest gratitude to my supervisors, Dr. Jessica Steinkopf and Prof. Francois Engelbrecht, for their continuous guidance, encouragement, and constructive feedback throughout this research. Their expertise and support have been instrumental in shaping this dissertation.

I am also grateful to the staff and fellow students at the School of Geography, Archaeology and Environmental Studies at the University of the Witwatersrand for creating a supportive and engaging academic environment.

To my family and friends – thank you for your unwavering support, patience, and motivation during this journey. Your belief in me has meant everything.

Abstract

This dissertation investigates the impact of the El Niño Southern Oscillation (ENSO) on rainfall variability over the eastern escarpment of South Africa, a key water source for surrounding regions. Using observational rainfall data from the Climate Research Unit (CRU) and ERA5 reanalysis, this study analyses annual and seasonal patterns in response to different ENSO phases, namely El Niño, La Niña, and neutral conditions, from 1981 to 2023.

The results show that there is significant regional variability, particularly in the eastern escarpment which tends to record higher annual rainfall compared to other parts of the country. Seasonal analysis of CRU data identifies the December-February (DJF) and September-November (SON) seasons as the wettest periods, whereas the June-August (JJA) season experiences the least rainfall. The results show a strong correlation between ENSO and rainfall variability, particularly during DJF, when El Niño events suppress rainfall, and La Niña phases enhance rainfall. Notably, the severe El Niño events of 1982/83 and 2015/16 led to severe drought conditions.

ERA5 data is found to closely align with CRU observations, successfully capturing seasonal rainfall patterns and interannual rainfall variability, though ERA5 data does slightly overestimate rainfall. Composite maps highlight spatial differences in rainfall anomalies associated with ENSO events, clearly identifying the eastern escarpment as one of the regions most impacted by ENSO. Rainfall anomalies are particularly pronounced over the eastern escarpment study site, when compared to the country as a whole, especially during DJF, with El Niño phases significantly rainfall, and La Niña phases enhancing it.

This study underscores the importance of understanding how ENSO shapes rainfall variability, with implications for water resource management, agricultural planning, and drought mitigation in South Africa. Improved forecasting of ENSO events could help reduce economic losses and societal impacts linked to extreme weather climates.

Table of Contents

Declaration 2

Acknowledgements 3

Abstract 4

Chapter 1: Introduction 9

Background 9

Rationale 11

Aim and Objectives 12

Structure of the Thesis 12

Chapter 2: Literature review 13

2.1 El Niño Southern Oscillation 13

2.2 ENSO indices 15

2.3 ENSO Predictions 17

2.4 Impact of ENSO on Global Climates 19

2.5 ENSO and the southern African Climate 22

2.6 Eastern Escarpment Mega-Dam Region and ENSO 24

Chapter 3: Data and Methodology 27

3.1 Study Site 27

3.2 Data 29

3.2.1 Rainfall Data 29

3.2.2 Niño 3.4 index 30

3.3. Methodology 31

3.3.1 Composite Anomaly Maps 31

3.3.2 Data Analysis 31

Chapter 4: Observational Data Analysis 33

4.1 Overview of CRU Data Analysis 33

4.2 Annual and Seasonal Rainfall Distribution and Variability 33

4.3 Quantifying the ENSO-Rainfall Relationship 38

4.4 Representation of the ENSO signal in CRU 44

Chapter 5: ERA5 Data Validation 48

5.1 ERA5 Rainfall Distribution and Variability 48

5.2 ERA5 Spatial Rainfall Biases 54

5.3 Statistical Insights into ERA5 and CRU data 56

5.4 Evaluating the ENSO-Rainfall Relationship in ERA5 59
5.5 Representation of the ENSO signal in ERA5 62
Chapter 6: Discussion 67
6.1 Introduction 67
6.2 Comparison between CRU and ERA5 Rainfall Distributions 67
6.3 ENSO-Rainfall Teleconnection: Implications and Variability 69
6.4 Regional Disparities in ENSO Impact 72
Chapter 7: Conclusion 75
7.1 Summary of Key Findings 75
7.2 Study Limitations and Future Research Directions 76
7.3 Final Thoughts 77
References 78

List of Figures

Figure 3.1: Study Area: South Africa with Eastern Escarpment 27
Figure 3.2: A map of the regions used for various Niño indices. 30
Figure 4.1: Spatial distribution of CRU total annual rainfall (mm) across South Africa, for the period 1979-2023, with the rectangular (red) box highlighting the study site. 33
Figure 4.2: Seasonal CRU rainfall totals (mm) across South Africa for 1981-2023, with the rectangular (red) box highlighting the study site. 36
Figure 4.3: Mean annual rainfall distribution across (a) South Africa and (b) the eastern escarpment study site for CRU, with mean (thicker dotted line) and standard deviations (thinner dotted lines). 38
Figure 4.4: Niño 3.4 Index for the DJF season for the period 1981 to 2023. 38
Figure 4.5: Spread in the seasonal rainfall anomalies, according to specific ENSO phases, across the eastern escarpment study site, for (a) DJF, (b) MAM, (c) JJA and (d) SON. Boxplots show the 25th, 50th and 90th percentiles, lines extending to minimum and maximum values and circles representing outliers. 41
Figure 4.6: Rainfall anomaly maps (mm) for DJF, associated with the ENSO cycle based on ENSO events between 1981 and 2023, for (a) El Niño, (b) La Niña and (c) Neural phases. Anomalies are calculated from the 1981-2023 average. 44
Figure 4.7: Rainfall anomaly maps (mm) for MAM, associated with the ENSO cycle based on ENSO events between 1981 and 2023, for (a) El Niño, (b) La Niña and © Neural phases. Anomalies are calculated from the 1981-2023 average. 45
Figure 4.8: Rainfall anomaly maps (mm) for JJA, associated with the ENSO cycle based on ENSO events between 1981 and 2023, for (a) El Niño, (b) La Niña and (c) Neural phases. Anomalies are calculated from the 1981-2023 average. 46
Figure 4.9: Rainfall anomaly maps (mm) for SON, associated with the ENSO cycle based on ENSO events between 1981 and 2023, for (a) El Niño, (b) La Niña and (c) Neural phases. Anomalies are calculated from the 1981-2023 average. 47
Figure 5.1: Spatial distribution in mean annual rainfall in the (a) ERA5 and (b) CRU data sets, for the period 1981-2023. Red box highlights the eastern escarpment study site. 48
Figure 5.2: Seasonal ERA5 rainfall totals (mm) across South Africa for 1981-2023 , with the rectangular (red) box highlighting the study site. 50
Figure 5.3: Mean annual rainfall distribution across the eastern escarpment study site for (a) CRU and (b) ERA5, with mean (thicker dotted line) and standard deviations (thinner dotted lines). 52
Figure 5.4: Interannual rainfall variability in the CRU (red line) and ERA5 (blue line) 52
data sets, across the eastern escarpment study site, for the period 1981 to 2023.
Figure 5.5: Interannual seasonal rainfall variability for CRU (black dotted line) 53
and ERA5 (red line), across the eastern escarpment study site.
Figure 5.6: Mean annual rainfall bias (mm) in the ERA5 data relative to CRU. 54
Figure 5.7: Seasonal bias in the ERA5 data relative to CRU for (a) DJF, (b) MAM, (c) JJA and (d) SON seasons. 55
Figure 5.8: The four quadrants investigated within the eastern escarpment study site. 56

Figure 5.9: Spread in the seasonal rainfall anomalies according to specific ENSO phases, across the eastern escarpment study site, for (a) DJF, (b) MAM, (c) JJA and (d) SON. Boxplots show the 25th, 50th and 90th percentiles, lines extending to minimum and maximum values and circles representing outliers. 59
Figure 5.10: Rainfall anomaly maps (mm) for DJF, associated with the ENSO cycle based on ENSO events between 1981 and 2023, for (a) El Niño, (b) La Niña and (c) Neural phases. Anomalies are calculated from the 1981-2023 average. 63
Figure 5.11: Rainfall anomaly maps (mm) for MAM, associated with the ENSO cycle based on ENSO events between 1981 and 2023, for (a) El Niño, (b) La Niña and (c) Neural phases. Anomalies are calculated from the 1981-2023 average. 64
Figure 5.12: Rainfall anomaly maps (mm) for JJA, associated with the ENSO cycle based on ENSO events between 1981 and 2023, for (a) El Niño, (b) La Niña and (c) Neural phases. Anomalies are calculated from the 1981-2023 average. 65
Figure 5.13: Rainfall anomaly maps (mm) for SON, associated with the ENSO cycle based on ENSO events between 1981 and 2023, for (a) El Niño, (b) La Niña and (c) Neural phases. Anomalies are calculated from the 1981-2023 average. 66

List of Tables

Table 4.1: Rainfall statistics per season across South Africa for the period 1981-2023 36
Table 4.2: Rainfall statistics per season across eastern escarpment study site, for the period 1981-2023
Table 4.3: Breakdown of ENSO years from 1981 to 2023 according to the Nino3.4 index 39
Table 4.4: Ranking of El Niño events and the associated area-averaged DJF rainfall anomalies across South Africa and the eastern escarpment study site. 42
Table 5.1: Rainfall statistics per season across South Africa for the period 1981-2023 50
Table 5.2: Rainfall statistics per season across eastern escarpment study site, for the period 1981-2023
Table 5.3: Statistical summary for seasonal rainfall for all quadrants in the eastern escarpment study site 58
Table 5.4: Ranking of El Niño and La Niña events across South Africa and the eastern escarpment study site, for the DJF season 61

Chapter 1: Introduction

1.1 Background

The El Niño Southern Oscillation (ENSO) plays a crucial role in the variability of global climate, influencing meteorological conditions worldwide annually through its extensive teleconnections (Trenberth and Hoar, 1997). It strongly influences year to year climate variability with significant global teleconnections which influence weather patterns across different regions (McPhaden et al., 2006). ENSO operates on a cycle that includes El Niño, La Niña, and Neutral phases, typically recurring every three to seven years (Meyers et al. 2007). During El Niño, sea-surface temperatures in the central and eastern Pacific rise above normal, whereas La Niña is characterised by below-normal sea-surface temperatures, as described by Meyers et al. (2007). Both events are driven by shifts in air pressure between the Australian-East Asian region and the eastern tropical Pacific, a phenomenon known as the Southern Oscillation, which influences atmospheric dynamics (McPhaden, 2008).

The impacts of ENSO on the global climate varies regionally, for example, in southern Africa El Niño events often lead to drastic drought conditions across the region, negatively impacting crop yields, and La Niña events often lead to enhanced rainfall, favouring crops to produce higher yields (Landman and Beraki, 2015). However, in eastern Africa the ENSO phases affect rainfall patterns differently. During an El Niño, wetter-than-normal conditions occur, which is beneficial for vegetation, and La Niña events result in below-average rainfall which leads to drought and reduced agricultural productivity (Anyamba et al., 2002). The variability in rainfall due to ENSO phases has direct influences on crop yields, food security and the livelihoods of the people, making ENSO a critical factor to consider when farmers conduct their agricultural planning (Benhin, 2006, McPhaden et al., 2006).

While ENSO events can have devastating impacts, there are examples of some economies around the world that benefited from these events. For example, according to McPhaden et al. (2006), the 1997-98 El Niño contributed $20 billion to the US (United States) economy due to reduced occurrences of hurricanes and the abrupt warm winter in the Midwest. Similarly, in southern and eastern Africa, ENSO-related climate variability has influenced agricultural activities, a sector that significantly contributes to the regional economy by accounting for 17% of the regional GDP (Gross Domestic Product)(Alemaw

and Chaoka, 2006; Nicholson, 2017). Understanding the links between ENSO events and rainfall patterns, particularly in regions like southern Africa where ENSO has such a strong influence, is vital. The influence of ENSO on rainfall and the consequent impact on people's livelihoods, emphasizes the need to understand and prepare for the different phases and their associated impacts.

Much research has been done on ENSO and it is thought that ENSO occurrences have been happening for the past 5 millennia (Enfield, 1992). However, it should be noted that the effects of ENSO are becoming more severe in various parts of the world. The Sixth Assessment Report (AR6) from the IPCC (Intergovernmental Panel on Climate Change) acknowledged that while there is uncertainty regarding future shifts in the strength and occurrence rates of El Niño and La Niña events, it is probable that the impacts associated with ENSO will intensify (Lee et al., 2021, Chapter 4, IPCC AR6 WGI). The intensification of ENSO phases is more noticeable across various regions in Eastern Africa, where ENSO is the prevalent factor which has worsened drought conditions, intensified food insecurity and affected the economic stability of these regions (Nicholson, 2017; Alemaw, 2022).

According to Lee and McPhaden (2010), an analysis of satellite data suggests that the intensity of El Niño events in the central equatorial Pacific has doubled in the recent three decades. Additionally, Lee and McPhaden (2010) obtained insights into the long-term patterns in the intensity of El Niño events and noted a significant increase in the intensity over recent decades. The gradual increase in the intensity of ENSO over the past several decades illustrates the need to further understand all aspects of this global phenomenon. Moreover, ENSO is recognized as the primary factor influencing drought occurrences in southern Africa, exhibiting a strong link between El Niño episodes and the region's precipitation patterns (Landman and Beraki, 2015). Grasping how this pattern and its effects in Africa might evolve with future climatic shifts is vital, carrying significant consequences for industry, development, policymaking, and societal structures. An improved understanding of ENSO events,specifically its link to drought occurrences, will contribute to planning and adaptation strategies. ness. While this study does not project future ENSO changes, identifying past ENSO-drought relationships is an important step toward better preparedness for potential ENSO-induced droughts.

1.2 Rationale

The eastern escarpment of southern Africa is a crucial region for water, given the large dams in this area supply water to the entire northern interior of South Africa, including Gauteng, the economic heartland of the country. Southern Africa is projected to become drastically warmer and likely drier under intensifying global warming (Ranasinghe et al., 2021). The associated water shortages in this region would have direct impacts on water supply and indirect impacts on the economy. This region experiences high interannual rainfall variability and the El Niño Southern Oscillation (ENSO) is a dominant driver of this variability (Nicholson and Kim, 1997). While the overarching connection between ENSO and southern African rainfall is well-documented, little research has been done on the specific influence of ENSO on rainfall over the eastern escarpment.

Furthermore, while some comparisons of different ENSO events exist, they often do not provide the granularity needed to understand local variances in climate response. This dissertation conducts a detailed comparative study of multiple ENSO events, exploring their distinct characteristics and differential impacts on rainfall specifically over the eastern escarpment. Developing our understanding of how rainfall in this region is impacted by ENSO is critically important for water security in the northern interior of South Africa, and especially for the agricultural sector, which is a major contributor to the economy and on which many livelihoods depend (Blamey and Reason, 2023). Knowledge gained in this project is crucial for informed water management, agricultural planning, and drought mitigation within such an essential water supply area.

Finally, ERA5 reanalysis data is used to benchmark many global climate models (GCMs). Given the importance of the ENSO-rainfall teleconnection in this region, it is crucial to assess how well the ERA5 outputs themselves capture the ENSO signal, when compared to observations. The analysis done in this dissertation will provide valuable inputs for future model analysis and development.

1.3 Aim and Objectives

The aim of this study is to investigate the role of the El Niño Southern Oscillation in rainfall variability over South Africa's mega-dam region. This is achieved through the following objectives:

- Quantify rainfall variability and its relationship to ENSO over the eastern escarpment region across all seasons, using observational data (CRU).
- Verify how well ERA5 reanalysis data captures the quantified ENSO-rainfall teleconnection over the eastern escarpment region.
- Understand how historical El Niño/La Niña events compare to one another in terms of their impact on rainfall over the mega-dam region

1.4 Structure of the Thesis

This thesis contains 7 chapters. This introductory chapter (Chapter 1) provides a brief overview of the research project, detailing the rationale, aim and objectives. Chapter 2 provides an extensive review of the relevant literature. Chapter 3 describes the study site, data used, and methodologies applied in the analysis. Chapters 4 and 5 are results chapters, first quantifying the ENSO-rainfall teleconnection using observational data and then verifying the reanalysis dataset (ERA5). Chapter 6 is the discussion chapter which provides an interpretation of the key findings from the results chapters. Finally, Chapter 7 is a concluding chapter that provides a synthesis of the study.

Chapter 2: Literature review

2.1 El Niño Southern Oscillation

The term El Niño was first introduced by Peruvian fishermen and was used during the late 19th century to explain the temperature changes along the coast, which had a negative impact on local fisheries. It was only during the 1960s when the broader understanding of El Niño Southern Oscillation (ENSO) was established, when Jacob Bjerknes surmised that the coastal El Niño events were connected to the broader atmospheric changes, now known as Southern Oscillation, and suggested that the Walker Circulation has a positive feedback role in the development of ENSO (Trenberth, 1997). Hence, the El Niño Southern Oscillation describes a complex and transient global phenomenon involving changes in both sea surface temperatures (SSTs) and global atmospheric circulation.

El Niño is used to refer to a weak warm ocean current that moves southward along the coast of Peru and Ecuador (Trenberth, 1997), where there are abrupt changes in the tropical Pacific SSTs, while the "Southern Oscillation" refers to the associated changes in the sea level pressure, overall describing this coupled ocean-atmosphere interaction (Trenberth, 1997). Hence, El Niño is the cyclical warming event affecting sea surface temperatures in the tropical Pacific, which occurs on average every two to seven years, but not necessarily in a regular cycle. As for La Niña, which is the opposite to El Niño, the phase consists of enhanced cooling in the central and eastern tropical Pacific, which is accompanied by strengthened trade winds and increased upwelling near South America (Lee and McPhaden, 2010). That is, it is characterised by cooler than normal SSTs in the Pacific, affecting global weather patterns (Glantz, 2002). During El Niño events, a significant amount of heat is transferred from the ocean to the atmosphere, specifically across the Pacific. This large transfer of heat influences the global weather patterns including global surface temperatures. With La Niña events, there is an increase in the heat absorbed by the ocean, contributing to different climatic effects (Lee and McPhaden , 2010). Hence, ENSO can have adverse effects on agriculture, water resources, and disaster management strategies across various regions across the world (Glantz, 2002).

The development of different ENSO phases is driven by coupled ocean-atmosphere interactions, with the Walker Circulation being a key component of these processes. Specifically, during neutral conditions, easterly trade winds traverse the tropical Pacific,

pushing warm surface water westward, accumulating this warmer water in the western Pacific, which causes cooler water to rise to the surface in the eastern Pacific through upwelling (Kessler, 2006). Over the warm water, air rises in the western Pacific, travels eastward at high elevations, and descends in the eastern Pacific, forming the Walker Circulation (Kessler, 2006).

When SSTs in the eastern Pacific rise, the temperature gradient between the east and west weakens, leading to a reduction in the strength of the trade winds and further weakening of the Walker Circulation (Lindzen and Nigam, 1987; Gill, 1980). Walker Circulation weakening causes the trade winds to slow down, disrupting ocean currents and raising the SSTs in the eastern Pacific. This results in El Niño conditions, the warm phase of ENSO, which is driven by coupled ocean-atmosphere feedback (McPhaden, 2008). The subsurface ocean dynamics also play a critical role in the development of El Niño events. The temperature anomalies across the subsurface originate from the western Pacific and propagate eastward, contributing to SST anomalies in the eastern Pacific. This process plays a crucial role in ENSO dynamics (Kessler (2006); Vecchi and Harrison (2006)).

Over time, the trade winds will strengthen again and can become even stronger than normal, pushing warm waters back into the western Pacific, while cool waters collect at the surface in the eastern Pacific (Philander, 2001). This results in La Niña conditions, characterized by unusually cold SSTs in the eastern Pacific and a strengthening of the Walker Circulation (Trenberth and Stepaniak, 2001; DiNezio et al., 2017). The transition between El Niño and La Niña conditions is irregular. Typically, ENSO events last nine to 12 months, but some events can occur for years (Trenberth and Stepaniak, 2001).

The transition from El Niño's warm phase to La Niña's cold phase was not well understood in Bjerknes's early studies (Philander, 2001). Not much was known about ENSO until the big El Niño event of 1982–1983, which was mostly ignored until it had serious impacts. Up until the late 1990s, there was far less focus on the impacts of La Niña compared to El Niño events. Only after the intense 1997-98 El Niño event, did the scientific community develop interest in forecasting techniques that predicted a strong La Niña for the summer of 1998. That is, following the 1997-98 El Niño, there was a drastic change towards building models that would predict the behaviour of La Niña events due to its global impact on weather systems (McPhaden et al., 2006). Advancements in research have led to a better understanding of the distinct impacts of La Niña compared to El Niño, specifically its

impact on the hydrological cycle and the responses in the ocean-atmosphere interactions (Trenberth and Stepaniak, 2001).

2.2 ENSO indices

Our understanding of ENSO dynamics has significantly improved since the early 1980s due to the development and increased use of different ENSO indices, such as the Southern Oscillation Index (SOI) and various SST indices (Niño 1, 2, 3, and 4), which have improved our ability to monitor and characterise ENSO events (Wang et al., 2017). Each Niño region responds differently to ENSO phases, reflecting variations in ocean-atmosphere interactions. The Niño 1+2 index captures early ENSO signals near the South American coast, while Niño 3 represents classical Eastern Pacific ENSO events (Hanley et al., 2003). The Niño 3.4 index is widely used to classify ENSO phases, as it provides insights into event intensity and duration. The Niño 4 index is more indicative of Central Pacific ENSO events, which have distinct climate impacts (Hanley et al., 2003).

The Niño 4 and Niño 3.4 indices respond differently to the different ENSO phases, with Niño 4 showing a weaker response to El Niño but a stronger response to La Niña, likely due to stronger cooling persistence in the central Pacific (Hanley et al., 2003). Furthermore, the Niño 3.4 index tends to be more symmetrical between El Niño and La Niña events, offering details about the duration and intensity of ENSO events, and is therefore a key indicator for ENSO monitoring. According to Hanley et al. (2003), the Niño 1+2 and Niño 4 indices are especially helpful in identifying ENSO patterns during the boreal winter season, which coincides with the austral summer rainfall season over southern Africa. When combined, these indices provide a comprehensive view of the complex seasonal and regional variability of ENSO occurrences.

Yu and Kao (2007) observed distinct decadal variations in the persistence barriers of the four Niño SST indices (Niño 1+2, Niño 3, Niño 3.4, and Niño 4). The persistence barrier, defined as the month when the lagged autocorrelation of an SST index drops significantly faster than in other months, indicating minimal persistence, varied across the indices. Specifically, for the central-Pacific indices (Niño 3.4 and Niño 4), these barriers consistently occurred in the boreal spring from 1958 to 2001. In contrast, for the eastern-Pacific indices (Niño 1+2 and Niño-3), the timing of these barriers shifted from decade to decade. This

suggests that SST evolutions in the central and eastern equatorial Pacific are influenced by differing physical processes (Yu and Kao, 2007).

The Niño 3.4 region, overlapping portions of the Niño 3 and Niño 4 regions, covers an area from 5°N to 5°S and 120° to 170°W (Barnston et al., 1997). This region was defined based on the stronger correlation between the Southern Oscillation Index (SOI) and SST anomalies compared to other Niño regions (Barnston et al., 1997). Timing also influences which ENSO characteristics are best captured by various indices. The Niño 3.4 index is widely used for identifying ENSO events. The Niño 3.4 index captures ENSO events as they develop in austral winter (JJA) and strengthen through austral spring (SON), reaching peak intensity in austral summer (DJF) (Trenberth and Stepaniak, 2001). Other indices, such as Niño 1+2, Niño 4, and the Japan Meteorological Agency (JMA) index, also track ENSO variability (Hanley et al., 2003), particularly during DJF when ENSO teleconnections are strongest (Chen et al., 2024).

According to L'Heureux et al. (2024), the Oceanic Niño Index (ONI) provides a three-month running mean of SST anomalies relative to a 30-year climatology. It monitors changes in SST in the equatorial Pacific, notably across the Niño 3.4 region. El Niño (warming) or La Niña (cooling) phases are identified by climatologists using a threshold of plus or minus 0.5°C for at least five consecutive overlapping 3-month seasons (L'Heureux et al., 2024). Changes in SSTs in the Niño 3.4 region are closely associated with significant changes in atmospheric circulation, making ONI a key tool for distinguishing between ENSO episodes (Wang et al., 2016). Specifically, a positive ONI indicates above-normal SSTs in the central equatorial Pacific during El Niño, while a negative ONI reflects below-normal SSTs during La Niña (Villalobos et al., 2023). Having said this, because of its strong link with the effects of the worldwide climate variability, the Niño 3.4 index is one of the most used ENSO measures and a crucial diagnostic tool in evaluations of the global climate model outputs, such as those reported in the most recent recent IPCC AR6 report (Lee et al., 2021, Chapter 4, IPCC AR6 WGI).

2.3 ENSO Predictions

Historical analyses of past ENSO events have contributed to improving predictive models, enabling skillful forecasts longer in advance (Chen and Cane, 2008; Latif et al., 1998; L'Heureux et al., 2024). However, future projections suggest that greenhouse warming could

alter ENSO characteristics, potentially increasing the intensity of ENSO events, while increasing uncertainty in ENSOs forecasts (Chen et al., 2024). ENSO forecasts rely on coupled ocean-atmosphere interactions, including SST anomalies, subsurface heat content, and shifts in the Walker Circulation (Latif et al., 1998). However, forecasting accuracy at seasonal and interannual timescales is still limited by challenges in simulating Pacific SST variability and its associated atmospheric dynamics (Saurral et al., 2020).

The intensity and frequency of various climatic events, such as heat waves, and hydrological events, such as floods and droughts, are regulated by ENSO occurrences, which have a major impact on global atmospheric circulation patterns (Yeh et al., 2018). Fisheries, agriculture, and ecosystems are all directly impacted by these occurrences, which have an influence on the environment and regional economies at different scales (Li et al., 2023). It is important to note that ENSO's impact is not uniform, as noted by Kao and Yu (2009), who illustrated that not all El Niño or La Niña events produce the same effects, which complicates the prediction of their impacts. For example, the predictability of ENSO impacts is influenced by seasonal fluctuations in heat stored in the tropical Pacific Ocean's upper layers, driven by wind, which in turn affects global atmospheric circulation. Despite these complexities, forecasting systems have become more sophisticated over time, allowing more accurate predictions (McPhaden, 2008). However, early ENSO-related events, such as the strong 1997–1998 El Niño, were not well forecast in terms of their commencement, severity, and duration (Barnston et al., 1999).

Beyond climate forecasts, ENSO is also used to assess global flood risk. The global impact of ENSO on flood risk is examined using sophisticated modeling frameworks, including hydrological, hydraulic, and impact models, which help to quantify how ENSO-driven rainfall anomalies influence flood hazards (Ward et al., 2014). These models demonstrate how ENSO phases can be used as a predictor of either increased or decreased flood risks in different regions. ENSO's impact on flood risks globally is significant, altering the intensity and likelihood of floods across different regions. Large anomalies in flood volumes caused by ENSO vary in intensity and severity across regions (Ward et al., 2014). This substantiates the need to integrate ENSO considerations into disaster risk analyses and policies (Ward et al., 2014) and to better forecast ENSO events.

Furthermore, forecasting river flow patterns and controlling water allocation to catchment areas depend on understanding the connection between ENSO and precipitation (Alemaw

and Chaoka, 2006). Such information is crucial for creating long-term, sustainable water-use strategies and reducing the detrimental effects ENSO events often have on economies and societies (McPhaden, 2008). This highlights the importance of better forecasting methods as they can help reduce the negative impacts of ENSO while making the most of its benefits. The more accurately we can predict ENSO, the better prepared we'll be to manage risks and protect climate-sensitive industries (Wang et al., 2017). To increase forecasting accuracy, interdisciplinary research combining data science, atmospheric science, and oceanographic methodologies has been used (Ye et al., 2018). These integrated approaches have enhanced the ability to detect ENSO variability earlier and with greater precision.

As a result of these efforts, novel methods for more effectively evaluating big datasets have been developed, improving the accuracy of climate models and ENSO-related forecasts. Hund et al. (2021) highlight the importance of advanced forecasting methods in mitigating ENSO's adverse effects by improving water resource management, optimizing agricultural planning, and enhancing hydropower operations. Using South America as an example, Hund et al. (2021) highlights that El Niño-induced precipitation changes can improve water availability, benefiting hydropower generation and agricultural productivity when effective forecasting strategies are in place. By improving ENSO forecasts, societies can transition from reactive responses to proactive climate adaptation, minimizing economic losses and optimizing potential gains.

ENSO is a major driver of year-to-year climate variability and affects weather patterns worldwide. Hence, it is very important that global climate models (GCMs) accurately represent ENSO to improve seasonal and decadal climate predictions. However, forecasting the intensity and frequency of ENSO events remains a challenge, partly due to uncertainties in ocean-atmosphere feedbacks and model biases (Lee et al., 2021, Chapter 4, IPCC AR6 WGI).

Recent improvements in GCMs – driven by stronger computing capabilities, a better grasp of ocean-atmosphere interactions, and higher model resolution – have led to more accurate ENSO simulations (Yeh et al., 2018). These improvements are essential for forecasting extreme weather events, particularly ENSO-driven droughts and floods. However, uncertainties occur regarding how ENSO will evolve under climate change. Improving ENSO predictions will enable for more effective adaptation strategies to be developed and enhanced resilience to climate extremes (Collins et al., 2010).

2.4 ENSO impacts on regional climate across the globe

ENSO is known to impact rainfall patterns across many geographical regions and significantly alter regional climates (Douville et al., 2021, Chapter 8, IPCC AR6 WGI). During El Niño, many regions around the world experience significant shifts in rainfall patterns. For example the western coasts of North and South America often receive high rainfall, , while areas like Indonesia and Australia receive significantly less rainfall (Douville et al., 2021, Chapter 8, IPCC AR6 WGI). In contrast, La Niña often tends to create relatively cooler conditions which creates above-average rainfall across the western Pacific and reduced rainfall in the eastern Pacific (Behera et al., 2005). Significant ENSO-related climate anomalies have also been observed in the United States and Europe (Lin et al., 2024). ENSO impacts extend beyond regional and global climate, affecting ecosystems around the tropical Pacific and the economies of multiple countries (Liu et al., 2023). For example, in the Galapagos Marine Reserve, ENSO-driven changes in SST affect marine ecosystems, fisheries productivity, and socio-economic conditions for small-scale fishers (Castrejón et al., 2024).

The rapid changes in rainfall due to these ENSO phases cause catastrophic outcomes such as flooding, droughts that extend for long periods of time, impacts on agriculture, and food security (Benhin, 2006; McPhaden, 2008). For example, the 1997–1998 El Niño event led to devastating droughts in Indonesia and Australia, while simultaneously causing extreme flooding in Peru and Ecuador (Bayer et al., 2014). Furthermore, ENSO has drastic impacts on marine ecosystems, where the enhanced SSTs due to El Niño significantly affects phytoplankton growth, which is part of the oceanic food chain. These influences cause disruptions in marine habitat, impacting biodiversity and the fisheries that rely on them for sustenance (Castrejón et al., 2024). For example, in Peru, the 1982–1983 and 1997–1998 El Niño events severely impacted the Peruvian anchovy fishery, one of the world's largest, as warm waters reduced nutrient upwelling and drastically cut fish stocks (Barber and Chavez, 1983). Similarly, in the western Pacific, the 2015–2016 El Niño event caused severe declines in tuna catches, significantly affecting the economies of Pacific Island nations such as Kiribati and the Solomon Islands (Bell et al., 2018).

ENSO is one of the primary factors that influence extreme weather events. For example, El Niño conditions contribute to increased cyclone activity in the central and eastern Pacific due to the presence of warmer SSTs and favorable atmospheric conditions. Simultaneously,

the resulting increase in vertical wind shear over the Atlantic suppresses tropical cyclone formation, reducing cyclone activity in that basin (Vecchi and Soden, 2007). During La Niña events, Atlantic hurricane activity increases due to reduced wind shear and warmer waters, heightening the likelihood of hurricanes impacting the Caribbean, Gulf of Mexico, and southeastern United States (Vecchi and Soden, 2007; Chen and Cane, 2008). In contrast, in the central and eastern Pacific, La Niña conditions generally lead to fewer hurricanes (Vecchi and Soden, 2007). In the Pacific, El Niño events significantly influence the frequency and trajectory of tropical cyclones. Central Pacific El Niño has been linked to increased tropical cyclone activity and landfalling storms in East Asia, particularly in China, Korea, and Japan (Pan et al., 2024).

The variability in rainfall due to ENSO events poses a risk and a significant challenge to the management of water resources. When drought conditions intensify, it can lead to destructive outcomes such as deforestation and land degradation (Binns et al., 2001). ENSO's activity dramatically influences global temperatures, which often cause anomalies that disrupt seasonal weather patterns. Lin et al. (2024) and Liu et al. (2023) highlight that during El Niño, Pacific SST anomalies modify atmospheric circulation, leading to warmer winters in the Northern Hemisphere. These shifts influence energy consumption patterns and agricultural productivity by altering precipitation and temperature distributions. Whereas, during La Niña events, cooler temperatures often prolong the duration of winter conditions, impacting heating demands and spring planting schedules for farmers in the Canadian Prairies and the Midwestern United States (Bonsal et al., 2001).

In southern and eastern Africa, agriculture is the primary economic activity, which contributes about 17% to the regional gross domestic product (GDP) and supports the livelihood of 60% of the region's population (Nhemachena et al., 2020). Given the importance of agriculture and the impact ENSO has on agriculture, these regions are particularly vulnerable to adverse ENSO effects. For example, in Ethiopia ENSO negatively impacts rainfall in the region, with the majority of droughts that have occurred within the past three decades, and resulted in major agricultural stress, occurring during strong El Niño events (Matewos, 2019). The climate in eastern Africa is strongly influenced by ENSO, where drought conditions have intensified and occurred for the past several decades during La Niña events, which has caused food insecurity to be rampant across the region (Qu et al., 2019). Between 2008 and 2010, the drought conditions in East

Africa were significantly worsened by ENSO which had impacted over 13 million people (Nicholson, 2017). Droughts of this scale have been linked to reduced agricultural production and declining water availability, exacerbating food insecurity and economic vulnerabilities across many regions (AghaKouchak, et al., 2015). Furthermore, East African countries often see an increase in rainfall during an El Niño, but when these intense downpours get too great, some areas may become susceptible to floods (Palmer et al., 2023).

2.5 ENSO and the southern African Climate

The distribution of rainfall across southern Africa, particularly in areas south of 10°S, shows relatively high variability across different temporal scales. The climate in this region follows a distinct seasonal cycle, with alternating dry and wet periods influenced by ocean-atmosphere interactions. During the austral summer months (December–February), significant rainfall variability is observed due to prevailing climate drivers (Crétat et al., 2010). An exception to this is rainfall in the southwestern Cape which peaks during the austral winter, and the Cape south coast of South Africa, which experiences rainfall throughout the year (Engelbrecht et al., 2015). According to Nicholson (2017), ENSO plays a key role in modulating interannual rainfall variability, affecting both the timing and intensity of seasonal precipitation patterns. Furthermore, the rate of evaporation is impacted by temperature fluctuations brought on by ENSO events, which in turn affects the amount of water resources available for agricultural uses. Additionally, the impact of ENSO on southern Africa's precipitation patterns is modulated throughout the wet season, with variability influenced by both daily atmospheric dynamics and interactions with other climate drivers such as the Indian Ocean Dipole (IOD). This complexity makes seasonal rainfall predictions more challenging Dieppois et al. (2015) .

The impacts of ENSO on rainfall on eastern and southern African regions are marked by differences in the rainfall patterns in these regions. For instance, during the strong El Niño event of 1997/98, regions in eastern Africa experienced high rainfall while in southern Africa extreme drought conditions were experienced and similar observations were made during other significant ENSO events (Anyamba et al., 2002). Recently, the 2023/4 El Niño brought severe flooding to East Africa, displacing at least 2 million people, causing loss of lives, and damaging critical infrastructure (OCHA, 2023). This followed the region’s most prolonged drought (2020–2023), driven by La Niña, which left millions

facing starvation and displacement (UNDRR, 2024). This dipole effect is elaborated in detail by Steinkopf and Engelbrecht (2022), where they clearly demonstrated, using ERA5 and ERA-Interim data, how dry conditions occur in southern Africa and wet conditions in East Africa during El Niño events and the opposite during La Niña events.

Apart from seasonal variations, rainfall in southern Africa also exhibits significant year-to-year fluctuations. The primary influence on this interannual rainfall variability is ENSO, affecting summer precipitation in particular by responding to changes in SSTs in the tropical Pacific Ocean (Behera et al., 2000). Historical records show that ENSO's impact on the southern African climate is not uniform. For example, during the 1877-1878 El Niño, various parts of southern Africa experienced contrasting weather conditions, highlighting the complexity of ENSO's impact on the region (Brugnara et al., 2023).

In southern Africa, conditions are usually drier than normal during El Niño years and wetter than normal during La Niña years (Blamey and Reason, 2023; Rouault et al., 2024; Steinkopf and Engelbrecht, 2022). Numerous studies consistently demonstrate that rainfall across southern Africa, particularly in South Africa, is typically below average from December to March during El Niño episodes (Dieppois et al., 2015; Rouault et al., 2024; Nicholson, 2017). However, according to a recent study by Mpheshea et al. (2025), not all El Niño events have the same effects on rainfall in the region. The distinction between the types of El Niño events is made according to the origin of the event. They noted that El Niño originating from the Eastern Pacific (EP) tends to have more severe impacts as compared to El Niño from the Central Pacific (CP).

ENSO's effects are not uniform across the region – different climatic and geographic settings cause summer and winter rainfall zones to respond differently (Brugnara et al., 2023). For instance, it has been noted that the Western Cape region of South Africa can have above-average winter rainfall during El Niño episodes, in contrast to the region as a whole, which generally exhibits dry conditions (Reason and Rouault, 2005). Furthermore, not all El Niño events result in drought conditions throughout the region. For instance, South Africa received normal to above-average rainfall during the 1997–1998 El Niño period, despite the fact that it caused drought conditions in several areas of southern Africa (Lyon and Mason, 2009). ENSO's impact is not isolated and is influenced by other large-scale phenomena. Specifically, the fluctuating SST anomalies, associated with El Niño, when combined with other climate parameters, such as wind patterns and ocean heat

content, result in varying rainfall characteristics, which contribute to the contrasting influence of ENSO (Kao and Yu, 2009). Furthermore, the way that ENSO influences the development of Tropical Temperate Troughs (TTT) is one of the main elements causing variability in the region. In regions like Botswana, Zimbabwe, and South Africa, these northwest to southeast cloud bands are a major contributor to the region's intense summer rainfall. Fewer TTTs form during El Niño years, which lowers rainfall and exacerbates drought conditions (Hart et al., 2018).

In examining how ENSO influences intra-annual rainfall cycles in southern Africa, Alemaw (2022) confirms a strong link between ENSO and DJF rainfall patterns. The study finds that in 40.5% of the region, higher Niño 3.4 values correlate with increased DJF totals, indicating a positive relationship between SST anomalies and seasonal precipitation. An additional 17.4% of the region shows a weaker but statistically positive correlation between the two variables. That is, it is further confirmed that during El Niño years, southern Africa tends to experience below average rainfall, whereas during La Niña years, there are above average rainfall conditions. Such rainfall patterns are more pronounced in regions across Zimbabwe, Namibia, South Africa, Botswana, and Zambia (Alemaw, 2022).

It is clear there is a well-established relationship between ENSO and rainfall over the broader southern African region. Given that fluctuations in rainfall have a direct impact on agriculture, where food security depends on seasonal precipitation, the forecast of ENSO-rainfall impacts are crucial for the agricultural sector. Variations in temperature and rainfall can have a significant impact on crop output, and consequently the broader economy (Benhin, 2006). El Niño years can result in widespread crop failures because of the dry weather, while La Niña years tend to have wetter conditions that improve soil moisture and increase agricultural output, although there is a risk of flood events. This highlights the importance of developing early warning systems and climate adaptation strategies to mitigate the risks associated with ENSO variability. Furthermore, the skill of seasonal forecasts is dependent on ENSO (Landman et al., 2001) and therefore it is crucial to fully examine the relationship between ENSO and rainfall in the region, especially a critical water-supply sub-region like the eastern escarpment.

2.6 Eastern Escarpment Mega-Dam Region and ENSO

The Maluti Mountains in Lesotho, southern Africa, form a prominent escarpment, with elevation that exceed 1000 metres between valley floors and adjacent peaks (Taylor et al., 2016). Mathinya et al. (2022) investigated patterns of precipitation and river discharge in the Maloti-Drakensberg region, highlighting significant variability in rainfall distribution. The study revealed that annual precipitation in the uThukela catchment ranges from approximately 600 mm in lower-lying areas to 2000 mm in high-elevation regions. Notably, rainfall increases with altitude, contributing to distinct precipitation patterns across different zones. The role of alpine wetlands and grasslands in regulating water flow and buffering against extreme rainfall events was also emphasized, as degradation of these ecosystems has led to increased variability in river discharge (Mathinya et al., 2022).

The eastern escarpment is a prominent geographical region, which serves an important role in the hydrological system of southern Africa. The escarpment separates the coastal areas and the interior plateau, acting as a blockade that allows it to control weather patterns and the distribution of rainfall across South Africa (Taylor et al., 2016). The barrier between the ocean and land causes air masses from the ocean to get uplifted as they encounter the escarpment. During its upliftment along the escarpment, the air mass cools down and releases moisture in the form of precipitation. This whole process is what allows regions along the escarpment to experience a large volume of convective rainfall in South Africa (Blamey and Reason, 2023). Lesotho's rainfall variability is strongly influenced by ENSO, which affects both inter-annual and seasonal precipitation trends (Nash and Grab , 2010; Hlalele and Makhubele, 2024).

Specifically, as with the broader southern African region, during El Niño (La Niña) events, Lesotho often experiences below-average (above-average) rainfall, (Hlalele and Makhubele, 2024). The Maluti-Drakensberg, has a highly elevated landscape and complex topography, which would exhibit increased sensitivity to climate variability, including interannual shifts associated with ENSO phases. However, the relationship between altitude and climate sensitivity is not fully understood. For example, Mbiriri et al. (2018) found that altitude plays a role in modulating drought patterns, but their results do not necessarily support the claim that altitude enhances all ENSO-related impacts. The local impacts of ENSO are strongly influenced by altitude, with higher elevations experiencing

pronounced climate fluctuations, including changes in snowfall patterns. Given that mountain ecosystems serve as vital water sources and support economic activities beyond their immediate boundaries, effective conservation and disaster management strategies are necessary to mitigate the vulnerability of the region to drought conditions (Mbiriri et al., 2018). Taylor et al (2016) highlight that the Lesotho highlands and the Drakensberg escarpment function as the so-called ‘water tower’ of South Africa, supplying major river systems that extend across the country.

The high-altitude topography of the escarpment allows for the slow distribution of water from high rainfall events, acting as a natural water reserve. The controlled release of water from reservoirs plays a vital role in regulating river flows, particularly during periods of low rainfall. Such regulation is crucial for maintaining downstream ecological balance, as it influences water temperature, oxygen levels, and sediment transport, all of which are critical for sustaining aquatic biodiversity and ecosystem functioning (Impson et al., 2007). However, recurring ENSO events, specifically strong El Niño phases, have been associated with severe droughts in southern Africa, posing risks to water security in Lesotho and South Africa (Alemaw, 2022; Brugnara et al., 2023).

The Lesotho Highlands Water Project (LHWP), which supplies water to South Africa, is highly sensitive to ENSO-induced fluctuations in seasonal rainfall (Hlalele and Makhubele, 2024). The project's extensive infrastructure, including major reservoirs such as Katse and Mohale, has led to its designation as a "mega-dam" region (Engelbrecht et al., 2020). These dams are strategically located in the remote mountainous areas of Lesotho, harnessing the water resources of the Senqu/Orange River system. Given the increasing hydroclimatic variability associated with ENSO and projected climate change, understanding future precipitation patterns is critical for adaptive water management strategies. As key water catchment areas, these mountain regions are legally protected in South Africa and Lesotho (Nel et al., 2013).

Beyond its unique geography that enhances water collection, the escarpment is also characterised by extensive grasslands and indigenous woodlands. The grasslands and woods of Lesotho are essential to preserving the water cycle. By allowing rainwater to seep into the soil, they restore subterranean supplies that local communities rely on for farming and drinking water (Binns et al., 2001). Water supplies are kept steady over time

by the dense plant cover, which slows down runoff, prevents soil erosion, and ensures that aquifers gradually refill. Lesotho's climate is highly variable , shaped over time by ENSO's shifting patterns. It has experienced both extreme droughts and destructive floods (Beharie, 2019), which has implications for water supply in the broader region, impacts livestock and can lead to food shortages.

Chapter 3: Data and Methodology

3.1 Study Site

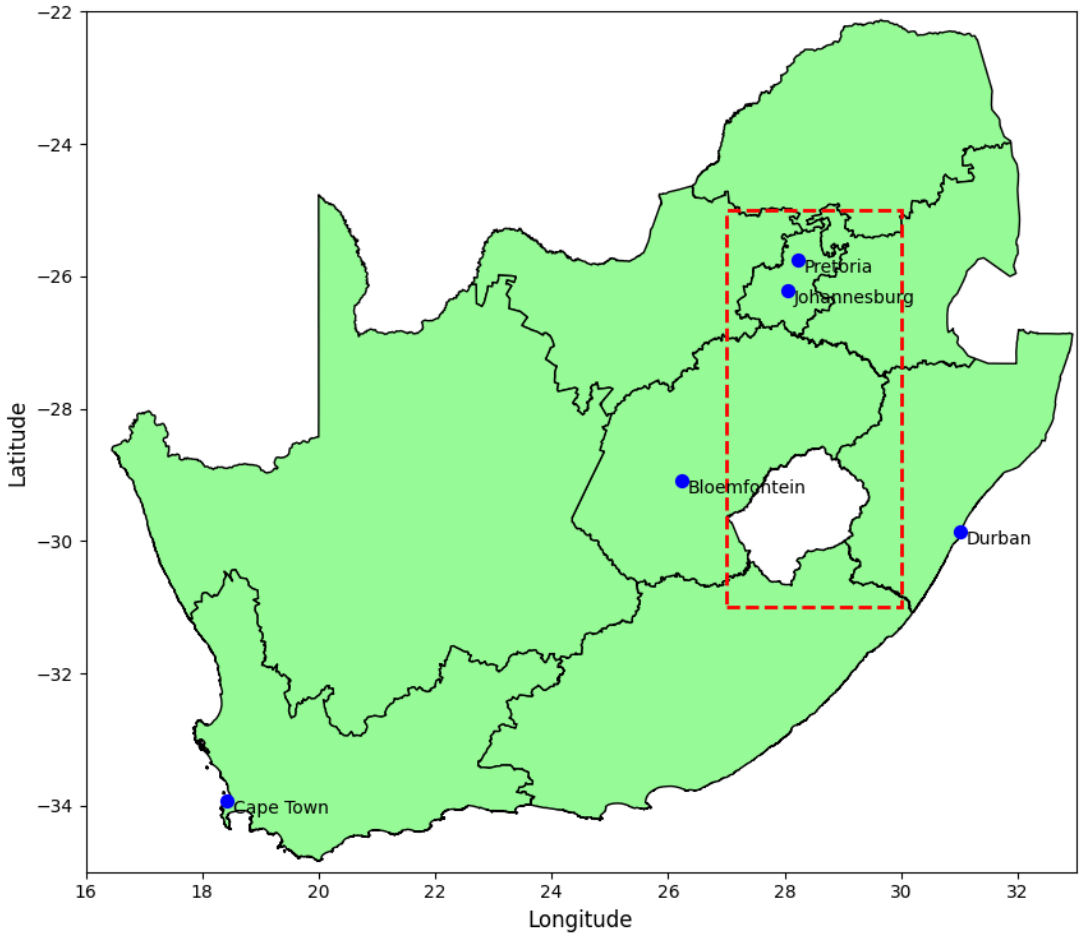

Figure 3.1: Study Area: South Africa with Eastern Escarpment

Semi-arid regions make up the majority of South Africa. However, due to its irregular geography, it features a variety of climates, from sub-humid and moist near the eastern shore to semi-arid and desert in the dry northwest (Benhin, 2006). The Orange-Senqu River, which drains water out of the Drakensberg mountains and empties into the Atlantic Ocean, has the largest catchment area, covering an area of around 100,000 km² (Taylor et al., 2016). Long-distance water transmission from the Orange-Senqu watershed of the Maloti-Drakensberg to a number of urban and irrigation farming locations has been made possible in the contemporary age (Earle et al., 2006).

This study concentrated on the eastern escarpment of southern Africa (as shown in Figure 3.1), a region that receives most of its rainfall in summer and is expected to experience significant drying due to future climate changes (Engelbrecht et al., 2015). The Drakensberg mountains range in elevation from 2000m to over 3000m above sea level. Being a summer rainfall region, it receives most of its rainfall between November and February, with annual average rainfall of 1000mm (Blamey and Reason, 2023). During the austral summer months, temperatures can range from 20°C to over 30°C. Winter months are cold, with common occurrences of snowfall at the higher elevations and where temperatures can drop below 0°C (Mbiririet al., 2018).

The mega-dam area within this escarpment is vital for water supply to South Africa's northern interior. Essentially, the Drakensberg area along the eastern escarpment is crucial for water provision across southern Africa. The Gauteng province, reliant on water from this region, is a major economic hub, home to 42 percent of the urban population, responsible for half of the country's industrial output, and up to 80 percent of its mining production (Bills, Illgner and Nel, 2001). With water resources being finite, the absence of adequate conservation measures could detrimentally affect both the economy and the broader population. Implementing drought mitigation strategies could help lessen these effects.

In focusing on the mega-dam area, particularly within the Drakensberg region of the eastern escarpment, this area underscores its essential contribution to water provision across southern Africa, including the economically pivotal Gauteng province. Rainfall across the southern African region is influenced by ENSO (Reason et al., 2006; Landman and Beraki, 2015), but it is important to further develop our understanding of the ENSO rainfall teleconnection in this sub-region. Given the finite nature of water resources, the absence of effective conservation and drought mitigation strategies could severely impact the economy and the well-being of the broader population. Therefore, understanding the nuances of ENSO's influence on this critical region's precipitation patterns becomes paramount, guiding the development of strategies to mitigate the adverse effects of climatic fluctuations.

3.2 Data

3.2.1 Rainfall Data

Rainfall is one of the primary variables impacting hydrology (Sazib et al., 2020). This study

relied on the Climatic Research Unit (CRU) TS (Harris et al., 2020) and ECMWF Reanalysis v5 (ERA5) data (Hersbach et al., 2020) to assess the impact of ENSO on precipitation variability in South Africa's mega-dam region. ERA5 was chosen over ERA5-Land as it provides near-coastal grid points and includes a wider set of atmospheric variables required for ENSO-related analysis (Hersbach et al., 2020). The study has investigated how ENSO affects rainfall patterns along the eastern escarpment, using rainfall records and the Niño 3.4 index spanning from 1981 to 2023 for analysis.

The latest version of the CRU TS (version 4.08) was acquired from the CRU website (CRU, 2023). This dataset offers a grid-based, station-derived time series of climate variables like temperature and precipitation, spanning from 1901 to present, at a 0.5° horizontal resolution (Harris et al., 2020). The CRU TS data, known for its high-quality climate variable measurements, has been employed in several studies (see Harris et al., 2020). Since the 2000s, this dataset has supported various research projects in Africa (e.g. Hersbach et al., 2020; Gleixner et al., 2020; Steinkopf and Engelbrecht, 2022) and has been shown to correctly capture many of the spatial and temporal characteristics of rainfall in Africa, and particularly southern Africa (Steinkopf and Engelbrecht, 2022). Additionally, CRU has the advantage of being spatially and temporally consistent to fully understand how ENSO has impacted rainfall over the mega-dam region, in-situ observations would usually be examined. However, due to challenges in accessing consistent, long term station records across study the area, the CRU dataset, which makes use of quality controlled historical station data, is used for the baseline assessment (Harris et al., 2020; Dedekind et al., 2016a; Crétat et al., 2010). Nonetheless, studies have shown that CRU rainfall estimates in southern Africa can be less reliable in areas with sparse station coverage, which can introduce biases in representing local rainfall variability (Harris et al., 2020; Gleixner et al., 2020).

The second part of this project involved an assessment of how well a reanalysis dataset captures the observed impact of ENSO on rainfall in this region. Specifically, the latest version of the European Centre for Medium-Range Weather Forecasts (ECMWF) ERA5 reanalysis dataset is evaluated. ERA5 merges model predictions with observational data, including both terrestrial and satellite sources (Hersbach et al., 2020). This dataset is an upgraded version from its predecessor, ERA-Interim (Dee et al., 2011) and has an improved spatial resolution (0.25° x 0.25°) and better temporal resolution. The dataset covers a wider period which spans from 1950 to present, with 137 vertical levels which provides a better representation of the atmospheric processes (Hersbach et al., 2020). ERA5 resolves some of

the biases that were in ERA-Interim, one of which is the overestimation of rainfall in tropical regions, and improved interannual variability (Hersbach et al., 2020). For instance, in East Africa, ERA5 decreases the biases observed across rainy seasons and provides an improved representation of spatial rainfall distribution during extreme years (Gleixner et al., 2020). For comparison, ERA5 data was re gridded onto the CRU grid using bilinear remapping, to allow for both datasets to have a consistent spatial resolution. Several studies have utilised this approach, especially when trying to understand climate dynamics and in assessments of ENSO's influence on water resource management (Hersbach et al., 2020; Steinkopf and Engelbrecht, 2022; Gleixner et al., 2020).

3.2.2 Niño 3.4 index

ENSO episodes are identified using a variety of measures and indices, with the Niño 3.4 index being a well-known index k for monitoring global climate changes associated with past teleconnections (Trenberth, 1997; Hanley et al., 2003). That is, the Niño 3.4 index is used to monitor and describe the ENSO cycle. Hence, this study used the Niño 3.4 index to define historical ENSO events. It is defined as the area-averaged SST anomalies over the Pacific Ocean's Niño 3.4 zone, which extends from 5°N to 5°S and from 120°W to 170°W (Figure 3.2). Specifically, the Niño 3.4 index was obtained from the National Oceanic and Atmospheric Administration (NOAA) website (NOAA, nd). Following the methodology of Steinkopf and Engelbrecht (2022), the Niño 3.4 index was averaged for December to February (DJF). When this seasonal average was over 0.5, it was considered an El Niño phase; when the DJF average Niño 3.4 index was below -0.5, it was considered a La Niña phase. When there was neither an El Niño nor a La Niña, neutral phases were identified. This 3-month DJF average was selected because it is when the ENSO signal is most pronounced.

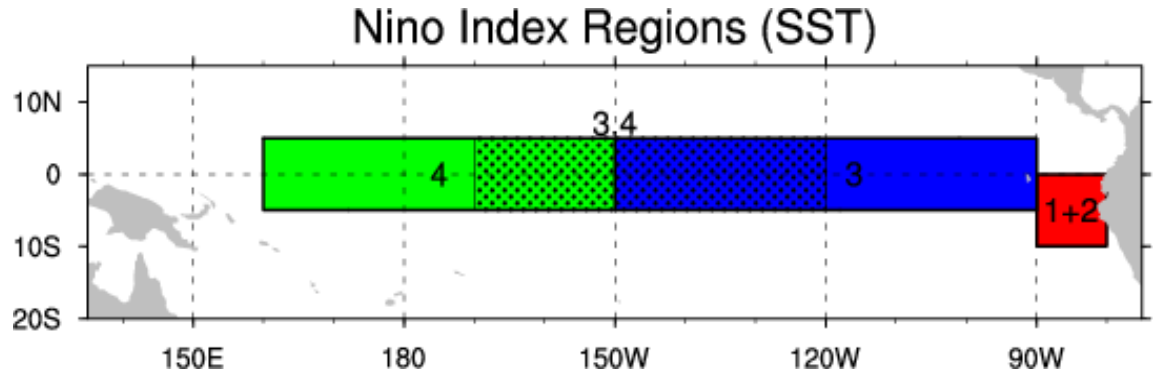

Figure 3.2: A map of the regions used for various Niño indices (UCAR, 2024).

3.3. Methodology

3.3.1 Composite Anomaly Maps

This study employed composite anomaly maps to capture the annual fluctuations in rainfall throughout southern Africa under El Niño, La Niña and neutral scenarios. These maps were constructed by calculating seasonal rainfall deviations from the long-term seasonal norm and then compiled these deviations for every instance of El Niño, La Niña and neutral phases. This method enabled an in-depth analysis of precipitation variances in the mega-dam region amid varying ENSO conditions. The study segmented the analysis by season – austral summer December to February (DJF), autumn March to May (MAM), winter June to August (JJA), and spring September to November (SON) with ENSO periods determined by the DJF averages of the Niño 3.4 SST anomalies (see Section 3.2.2). The ENSO phase associated with the other seasons was identified as follows: the JJA and SON before the DJF were classified as part of the event, whilst the MAM after was considered part of the same DJF event (Steinkopf and Engelbrecht, 2022). For example, if DJF of 2015/16 was identified as an El Niño, the preceding JJA and SON of 2015 were also El Niño and the following MAM of 2016 was an El Niño. The creation and examination of composite anomaly maps was done for both the CRU and ERA5 datasets. This enabled for another verification of the ERA5 dataset, given that the composite anomaly plots could be used to understand how well EAR5 captured the expected ENSO-rainfall signal that was observed in the CRU composite plots.

3.3.2 Data Analysis

Rainfall data were analysed using descriptive statistics, including mean, minimum, maximum, and standard deviation, to understand the rainfall distribution. These metrics provided a comprehensive understanding of the central tendency and spread of the data, while also identifying any extreme values (outliers) that would potentially distort the analysis. These calculations were done for both the whole of South Africa and the eastern escarpment. The analysis was undertaken for different temporal scales: yearly, seasonal and monthly. Time-series analysis was used to investigate temporal variability at both the monthly and seasonal levels. This included composite grouping of ENSO phases, visual inspection through line plots, and statistical association using Spearman's rank correlation. The calculations and analysis of these metrics was done using the following Python libraries throughout the analysis: xarray, netCDF4, numpy, pandas (for handling and processing climate and tabular data), scipy.signal, matplotlib and seaborn (for data visualisation), cartopy (for geospatial plotting), and geopandas and shapely (for vector based spatial operations and regional masking).

To ensure an accurate comparison between the observational and modelled outputs, bilinear remapping was used to regrid the EAR5 data onto the same 0.5° by 0.5° grid as the CRU data. Specifically, the remapping module of the Climate Data Operators (CDO) was used to regrid the data (Schulzweida, 2021). To understand the similarities and differences between the ERA5 and CRU datasets, annual and seasonal rainfall patterns were compared. Additionally, bias plots were created for all seasons and used to identify regions where ERA5 is over- or under-estimating the seasonal rainfall totals. Furthermore, rainfall data was arranged according to ENSO phases that were identified using the Niño 3.4 index (see Section 3.2.2). This approach simplified the process of identifying differences in rainfall patterns across each ENSO phase. For instance, rainfall anomalies during different El Niño years could be compared to each other and between the two data sources, enabling for a more detailed understanding of how different historical ENSO events compared to each other and further verification of ERA5 against the observations.

To explore the relationship between ENSO and rainfall variability, correlation and regression analyses were done. Spearman's Rank Correlation, a non-parametric statistical test, was used to determine the strength and direction of the relationship between the ENSO index (Niño 3.4) and area-averaged rainfall anomalies. This method assesses the monotonic

association between two variables without assuming a normal distribution, making it well-suited for analyzing climatic data (Spearman, 1904). The analysis was focused on the seasonal and annual time periods to study ENSO's influence on rainfall. To determine if the El Niño or La Niña periods were linked to wetter or drier conditions, the correlation values were analyzed. Furthermore, using Niño 3.4 index and historical data for CRU and ERA5, an analysis was conducted to study the statistical relationships between ENSO phases and rainfall patterns. The investigation included visual inspection of the time series plots, which showed periods of significant variation in rainfall patterns across time. In addition, we used histogram plots to visualise annual precipitations for South Africa and for the eastern escarpment, computed separately for CRU and ERA5 to summarise central tendency, dispersion, and skewness and to screen for outliers. Precipitation distributions were also arranged according to ENSO phases (El Niño, La Niña, and neutral years) to assess the regularity and variability of rainfall patterns during each of these periods. The Niño 3.4 index was selected for ENSO classification following the methodology of Steinkopf and Engelbrecht (2022).

In summary, the methodology offers a clear way to investigate the relationship between the eastern escarpment rainfall variability and ENSO in South Africa, with a particular focus on the eastern escarpment region. Through the use of CRU and ERA5 rainfall datasets and the Niño 3.4 index for sea surface temperature anomalies, we carried out a thorough study of the intricate relationship between ENSO and rainfall. We improved our understanding of this association by applying statistical analysis and the creation of composite anomaly maps.

Chapter 4: Observational Data Analysis

4.1 Overview of CRU Data Analysis

Chapter 4 explores the distribution of rainfall along the eastern escarpment by using a gridded observational dataset from the Climatic Research Unit (CRU) to establish and understand the influence of ENSO events on rainfall in this region. The chapter seeks to identify variations in rainfall patterns across different temporal scales and across different spatial scales (South Africa versus the eastern escarpment). By using the Niño 3.4 index, the ENSO-rainfall teleconnection is investigated. Correlation analysis is used to examine how ENSO phenomena affect rainfall in the region, providing a foundational overview of spatial and temporal trends that are further explored in subsequent chapters.

4.2 Annual and Seasonal Rainfall Distribution and Variability

Annual rainfall totals across South Africa show significant regional variability. The well-known west-east rainfall gradient in South Africa is clearly evident (Figure 4.1). In the country's eastern region, particularly around the eastern escarpment, mean annual precipitation is notably higher, typically 600mm and above per annum (Figure 4.1), while in the western regions mean annual precipitation is much lower, less than 300mm per annum (Figure 4.1). Notable exceptions are parts of the Western Cape region and the southeastern Cape coast, which both receive 500mm to 800mm of rain per year (Figure 4.1). The eastern escarpment region is characterized by relatively high annual rainfall totals with spatial heterogeneity. Mean annual rainfall increases from north (600-700mm) to south, especially the southeastern extent (800mm and above), with an average of 624.93 mm of rain per annum over the eastern escarpment study site (Figure 4.1, red box).

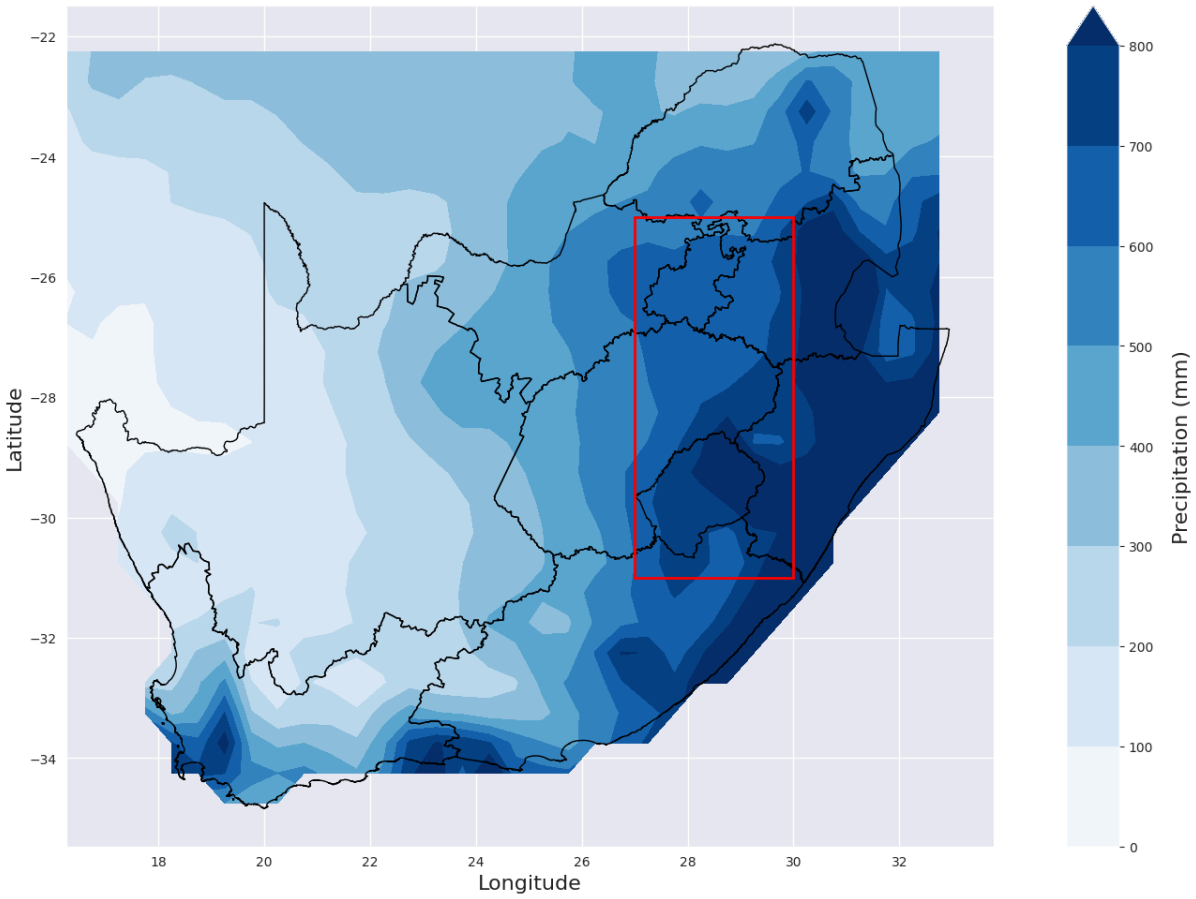

Figure 4.1: Spatial distribution of CRU total annual rainfall (mm) across South Africa, for the period 1981-2023, with the rectangular (red) box highlighting the study site.

Rainfall in South Africa is marked by large seasonal variability across different regions. The eastern region of South Africa receives most of its rainfall during the austral summer, December-January-February (DJF), and austral spring, September-October-November (SON), seasons, while the southwestern Cape region receives most of its rainfall during the austral winter, June-July-August (JJA), and austral autumn, March-April-May (MAM), seasons (Figure 4.2). Along the southwestern parts of the Eastern Cape, rainfall occurs throughout the year (Figure 4.2). Seasonal rainfall totals averaged across South Africa are highest during DJF (157.03 mm, Table 4.1), with a maximum of 1086.0 mm recorded on the eastern extent of the country (Table 4.2), and also highly variable (standard deviation of 138.79 mm). Consistent with the country-wide analysis, across all four seasons, seasonal rainfall over the eastern escarpment is highest in DJF (average of 320.43 mm), with a maximum of 1086.0 mm and minimum of 0 mm recorded over this period (Table 4.2). DJF

rainfall over the study site is also highly variable compared to other seasons (standard deviation of 147.92 mm, Table 4.2).

During the MAM season, rainfall totals over the southwestern region start to increase, while totals decrease over the eastern extent (Figure 4.2). The average MAM rainfall across the country drops to 86.39 mm and is less variable (standard deviation of 67.81 mm), with a maximum of 565.20 mm (Table 4.1). While total seasonal rainfall over the eastern escarpment does decrease during MAM, the season is not as dry as JJA (Figure 4.2). The average MAM rainfall over the eastern escarpment is 143.69 mm, with a maximum of 565.20 mm and a minimum of 0 mm (Table 4.2), which is less variable as was noted across the entire country. It is notable that for DJF and MAM the maximum value recorded in the eastern escarpment study site is the same as the maximum across the entire country.

During the period 1981-2023, South Africa experienced its lowest spatially averaged seasonal rainfall during JJA, making it the climatologically driest season country-wide (mean = 30.29 mm, standard deviation of 54.13 mm, Figure 4.2, Table 4.1). While northern parts of the country received little to no rainfall during JJA, the maximum average JJA rainfall of 585.80 mm (Table 4.1) was recorded in the western region of the country. Considering the eastern escarpment, across all four seasons, JJA is characterised by the lowest average rainfall, with the least variability (40.62 mm, standard deviation of 40.66 mm), ranging from a minimum of 0 mm to a maximum of 515.80 mm (Table 4.2). It is notable that in both JJA and MAM, rainfall across the eastern escarpment displays a north-south gradient, similar to the mean annual totals (Figures 4.1 and 4.2).

The SON season is characterised by increasing rainfall totals over the country as a whole and the eastern escarpment study site (Figure 4.2), making it the next highest contributor to annual rainfall totals after DJF. South Africa receives 85.17 mm of rainfall on average (standard deviation of 89.03 mm) during SON, with a minimum of 0 mm and maximum of 686.10 mm(Table 4.1), reflecting the seasonal nature of rainfall patterns reported across South Africa (Rouault et al., 2024). Over the eastern escarpment study site, the average seasonal rainfall during SON is higher and more variable than the country average, at 194.31 mm (standard deviation of 102.29 mm), with minimum and maximum values of 0 mm and 644.40 mm, respectively (Table 4.2). This highlights that DJF and SON are the wettest seasons, while JJA remains the driest, particularly in the eastern escarpment. Additionally, variability is highest in DJF and SON, as seen in their larger standard

deviations, whereas JJA exhibits lower variability, consistent with the region's dry conditions.

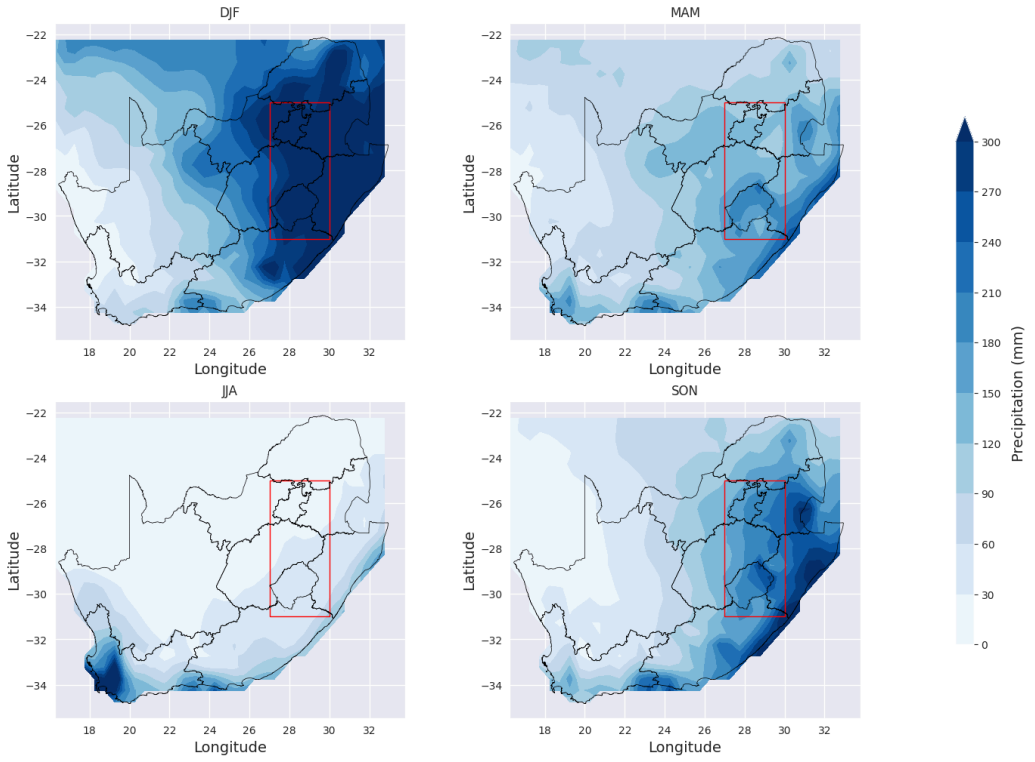

Figure 4.2: Mean seasonal CRU rainfall totals (mm) across South Africa for 1981-2023, with the rectangular (red) box highlighting the study site.

Table 4.1: Rainfall statistics per season across South Africa for the period 1981-2023

Season	Mean	Minimum	Maximum	Standard Deviation	25th Percentile	Median (50th)	75th Percentile
DJF	157.03	0	1086	138.79	34.3	131.2	248.7
MAM	86.39	0	565.2	67.81	38.4	79.2	121.2
JJA	30.29	0	585.8	54.13	1.3	8.9	35.73
SON	85.17	0	686.1	89.03	15.9	58.7	126.7

Table 4.2: Rainfall statistics per season across eastern escarpment study site, for the period 1981-2023

Season	Mean	Minimum	Maximum	Standard Deviation	25th Percentile	Median (50th)	75th Percentile
DJF	320.43	0	1086	147.92	259	332.9	401.7
MAM	143.69	0	565.2	77.15	99.08	141.3	189
JJA	40.62	0	515.8	40.66	13.08	30.4	55.4
SON	194.31	0	644.4	102.29	134.67	196.4	262.13

The rainfall distribution over South Africa and the eastern escarpment is shown in Figure 4.3. The distribution provides an overview of how rainfall is spread across these regions. South Africa (Figure 4.3a) receives a mean annual rainfall of 429.60 mm, with high variability (SD1: ±260.45 mm), indicative of the well-known uneven distribution of rainfall across the country. Most of the country receives relatively lower rainfall, with certain regions receiving significantly higher rainfall totals. In contrast, the eastern escarpment (Figure 4.3b) receives a higher mean annual rainfall of 706.75 mm, nearly double that of South Africa.

The rainfall in the eastern escarpment is shown to be more symmetric and bell-shaped, indicating that rainfall is more evenly spread across the area. The lower variability in rainfall over the eastern escarpment (SD1: ±156.37 mm) is not surprising given that the study site is a smaller region that falls within the same summer rainfall zone. The higher density around the 600-800 mm range suggests that most areas within the study site receive similar levels of rainfall, leading to a more uniform annual precipitation pattern. The differences in rainfall distributions highlight the need for subregion water resource planning and management, and the need to investigate ENSO-driven changes at a smaller scale.

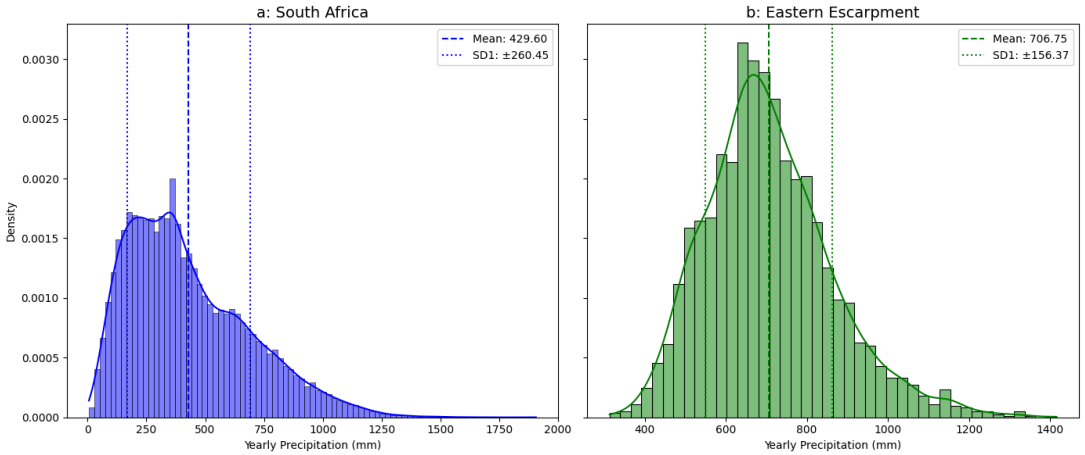

Figure 4.3: Mean annual rainfall distribution across (a) South Africa and (b) the eastern escarpment study site for CRU, with mean (thicker dotted line) and standard deviations (thinner dotted lines).

4.3 Quantifying the ENSO-Rainfall Relationship

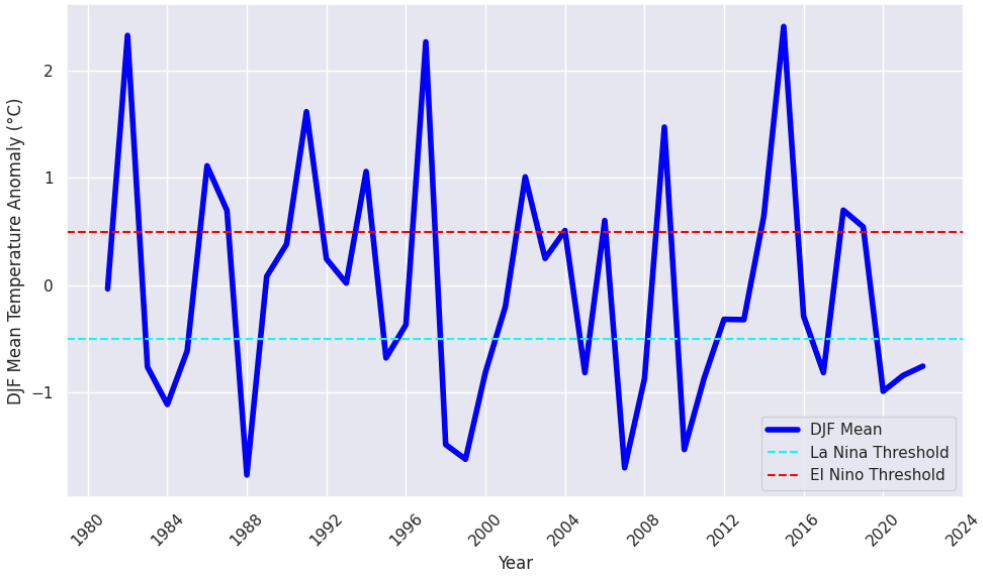

Figure 4.4: Niño 3.4 Index for the DJF season for the period 1981 to 2023.

ENSO is a major driver of rainfall variability in southern Africa. The climate system, during the time 1981-2023, oscillated between El Niño, La Niña, and neutral events (Figure 4.4). A number of El Niño events are visible in Figure 4.4, with a notable event occurring in the early 1980s, 1998, 2010, and 2015 when the SST anomalies were notably large. Furthermore, many La Niña events have occurred, including the most prominent ones in the

mid-1980s, early 2000s, and late 2010s, where the maximum SST anomalies are apparent (Figure 4.4). In reference to the Niño 3.4 index described in Chapter 3, the identified and analysed ENSO events in this study are listed in Table 4.3.

Table 4.3: Breakdown of ENSO years from 1981 to 2023 according to the Nino 3.4 index

Season	**El Niño Years**	**La Niña Years**	**Neutral Years**
DJF	1982/3, 1986/7, 1987/8, 1991/2, 1994/5, 1997/8, 2002/3, 2004/5, 2006/7, 2009/10, 2014/5, 2015/6, 2018/9	1983/4, 1984/5, 1985/6, 1988/9, 1995/6, 1998/9, 1999/2000, 2000/1, 2005/6, 2007/8, 2008/9, 2010/1, 2011/2, 2017/8, 2020/1, 2021/2, 2022/3	1981/2, 1989/90, 1990/1, 1992/3, 1993/4, 1996/7, 2001/2, 2003/4, 2012/3, 2013/4, 2016/7, 2019/20
SON/JJA	1982, 1986, 1987, 1991, 1994, 1997, 2002, 2004, 2006, 2009, 2014, 2015, 2018	1983, 1984, 1985, 1988, 1995, 1998, 1999, 2000, 2005, 2007, 2008, 2010, 2011, 2017, 2020, 2021, 2022	1981, 1989, 1990, 1992, 1993, 1996, 2001, 2003, 2012, 2013, 2016, 2019
MAM	1983, 1987, 1988, 1992, 1995, 1998, 2003, 2005, 2007, 2010, 2015, 2016, 2019	1984, 1985, 1986, 1989, 1996, 1999, 2000, 2001, 2006, 2008, 2009, 2011, 2012, 2018, 2021, 2022, 2023	1982, 1990, 1991, 1993, 1994, 1997, 2002, 2004, 2013, 2014, 2017, 2020

The spread in the rainfall anomalies at the individual grid points across the eastern escarpment study site (Figure 4.5) indicate that there are some regional responses to ENSO phases with large differences in magnitude and variability. The eastern escarpment study site tends to have high variability in the ENSO-induced rainfall anomalies, particularly for the DJF and SON seasons. The presence of many outliers is not surprising given this is a grid

point analysis and there is likely much variability both spatial and temporally across different ENSO events.

The below-average rainfall that is prominent over the region during El Niño events and above-average rainfall during La Niña events, is clearly evident in the boxplots for DJF (Figure 4.5a). It is notable that the negative anomalies during El Niño summers (DJF) are more prominent than the positive anomalies during La Niña summers (DJF). That is, there is a stronger response in the rainfall to El Niño events than La Niña events (Figure 4.5a). The boxplots also show a large number of outliers during La Niña DJF, further confirming the extreme nature of ENSO-related rainfall impacts during peak summer. While these anomalies are presented as absolute values, it is important to note that their relative significance can differ substantially depending on the regional climatology. For example, a 100 mm anomaly in a drier area may have a much greater impact than the same anomaly in a wetter region. Across all seasons there are some grid boxes with positive anomalies during El Niño's and negative anomalies during La Niña's. Considering the median of the spread, MAM and SON El Niño's are still predominantly drier than normal, with the signal of wetting less prominent during La Niña events (Figure 4.5b and d). The closer clustering of anomalies around zero in MAM and JJA indicates weaker anomalies during these seasons (Figure 4.5b and c). Additionally, the smaller differences in quantile values across ENSO phases suggest a much weaker ENSO teleconnection to rainfall during these periods. The reduced number of outliers in JJA further highlights ENSO's limited role during the dry season.

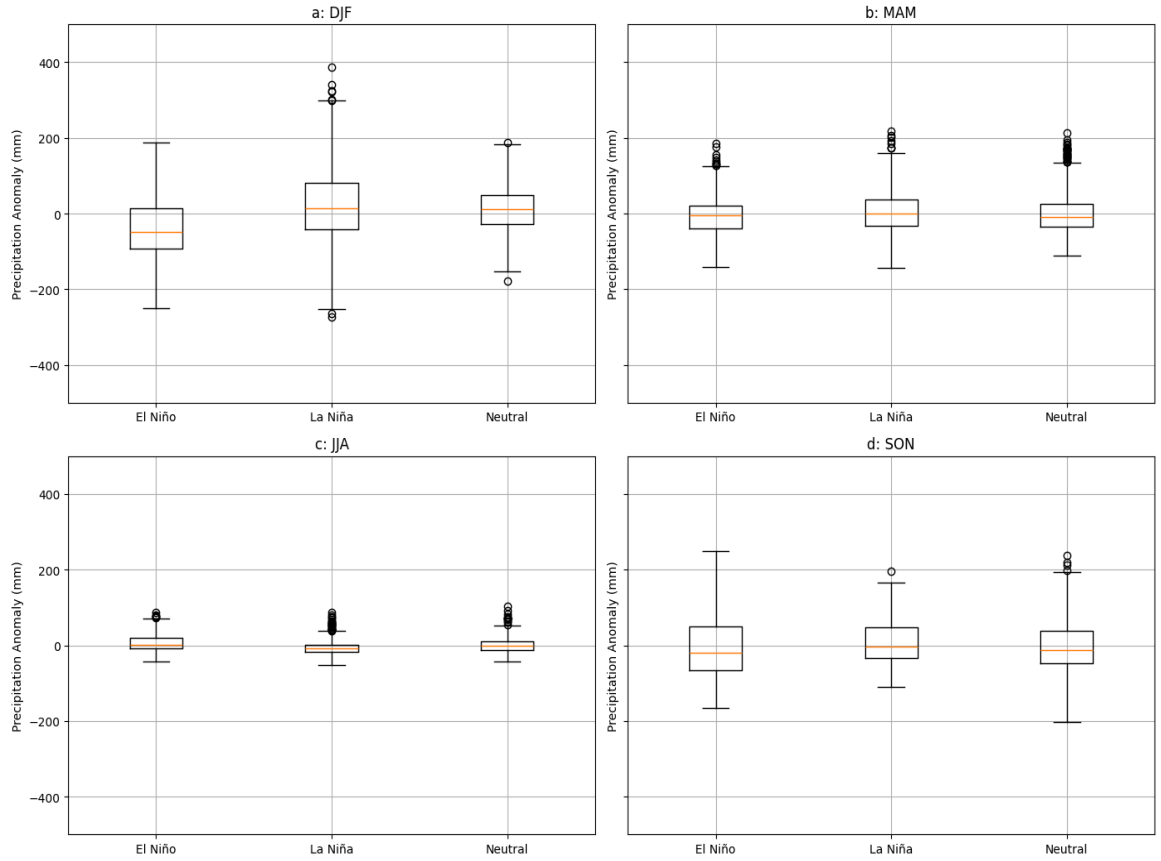

Figure 4.5: Spread in the seasonal rainfall anomalies, according to specific ENSO phases, across the eastern escarpment study site, for (a) DJF, (b) MAM, (c) JJA and (d) SON. Boxplots show the 25th, 50th and 75th percentiles; whiskers extend to the most extreme values within 1.5 X IQR from the lower and upper quartiles; circles represent outliers beyond this range.

Table 4.4: Ranking of El Niño events and the associated area-averaged DJF rainfall anomalies across South Africa and the eastern escarpment study site.

Ranked El Niño Year	DJF Niño 3.4 index (El Niño)	DJF rainfall anomaly South Africa (El Niño)	DJF rainfall anomaly Eastern Escarpment (El Niño)	Ranked La Niña Year	DJF Niño 3.4 index (La Niña)	DJF Rainfall Anomaly South Africa	DJF Rainfall Anomaly Eastern Escarpment
2015/6	2.41	-30.59	-104.97	1988/9	-1.77	91.89	188.39
1982/3	2.33	-67.64	-141.3	2007/8	-1.7	-1.72	-41.2
1997/8	2.27	-7.19	48.04	1999/0	-1.62	102.68	188.39
1991/2	1.62	-58.71	-90.2	2010/1	-1.53	38.27	86.7
2009/10	1.47	-44.91	66.64	1998/9	-1.48	-7.89	-29.13
1986/7	1.11	-37.83	-53	1984/5	-1.11	-27.42	-84.0
1994/5	1.06	-16.73	-62.17	2020/1	-0.99	9.73	35.02
2002/3	1.01	13.38	-26.96	2008/9	-0.87	28	48.99
2018/9	0.7	-21.99	-43.22	2011/2	-0.86	-10.11	-53.29
1987/8	0.7	33.68	-2.57	2021/2	-0.84	29.74	41.01
2014/5	0.64	-23.02	-53.59	2005/6	-0.81	41.04	55.6
2006/7	0.6	-33.84	-65.31	2000/1	-0.81	-20.17	-23.31
2004/5	0.51	11.48	26.62	2017/8	-0.81	-4.26	-20.42
				2022/3	-0.75	28.66	46.52
				1995/6	-0.68	45.49	126.20
				1985/6	-0.61	-27.79	-76.52

The table illustrates how summer (DJF) rainfall anomalies across South Africa and the eastern escarpment respond to different El Niño and La Niña events, ranked by the Niño 3.4 index. Overall, the results reinforce the well-established relationship between ENSO and rainfall in South Africa, with El Niño events generally associated with negative rainfall anomalies (drier conditions) and La Niña events with positive anomalies (wetter conditions). However, the magnitude of these anomalies varies between events, highlighting the complexity of ENSO impacts. The driest El Niño across both South Africa and the eastern escarpment study site occurred in the summer of 1982/83, with the second driest being the well-known 2015/16 event. These are the two strongest El Niño events based on the Niño 3.4 index (Table 4.4). 1991/2 was also an extreme case that resulted in widespread below-normal rainfall conditions both country-wide and over the eastern escarpment study site. It is notable that in all three of these cases, the drying effect was larger over the eastern escarpment study site than the country as a whole. This suggests that stronger El Niño events tend to exacerbate drought conditions, particularly in the key water-producing regions of the eastern escarpment. However, the 1997/8 and 2009/10 events are exceptions, with drying persisting over the country, but positive anomalies present over the eastern escarpment study site (Table 4.4). It is also interesting to note positive anomalies for both South Africa and the eastern escarpment study site during the weak El Niño event of 2004/5. This suggests that not all El Niño events uniformly lead to extreme drought.

Additional insights are derived when comparing the impacts of individual La Niña events on rainfall anomalies. There appears to be greater variability in the rainfall response during La Niña events, with almost half the events recording positive anomalies and the rest having negative anomalies (Table 4.4). Two of the strongest La Niña events of 1988/9 and 1999/2000 produced substantial positive rainfall anomalies across South Africa (91.89 mm and 102.68 mm, respectively), with particularly pronounced increases over the eastern escarpment study site (188.39 mm and 188.39 mm). Interestingly, the 2022/3 La Niña event was one of the driest years across both South Africa and the eastern escarpment, with -87.75 mm and -180.24 mm, respectively, but it was also one of the weakest events in terms of the Niño 3.4 index. However, some La Niña years (e.g., 2022/3, 1983/4 and 2011/2) show negative rainfall anomalies, suggesting that not all La Niña events guarantee widespread wet conditions. The 2022/3 La Niña stands out as an extreme case, with a strong drying signal (-87.75 mm across South Africa and -180.24 mm over the eastern escarpment study site). The magnitude of ENSO's impact on the eastern escarpment appears larger than in South

Africa, as shown in the stronger anomalies (both negative and positive). Interannual variability is evident, as some El Niño and La Niña years deviated from the typical rainfall patterns, likely due to other climate drivers.

4.4 Representation of the ENSO signal in CRU

Composite plots of the various ENSO events that occurred between 1981 and 2023 were created and are shown in Figures 4.6-4.9 below. The composite plots provide an illustration of the impact of ENSO phases on seasonal rainfall. During DJF, the well-known ENSO signal of dry conditions persisting over southern Africa (South Africa, Lesotho and Eswatini) during El Niño events and wet conditions persisting during La Niña events is clearly evident in the CRU observations (Figure 4.6). The negative anomalies are particularly strong in the eastern half of the country and weaker closer to the western coastal region and along the southwestern coastal region (Figure 4.6a). Strong drying is present across all the eastern escarpment study sites during the El Niño events. During La Niña events, the reversed signal of wetting is clearly shown by the positive anomalies. Similar to El Niño, the anomalies are stronger in the eastern part of the country and weaker in the western parts (Figure 4.6b). For the eastern escarpment study site, above-normal rainfall persists during the La Niña phase. Anomalies during the Neutral phase are generally weaker in amplitude and show more spatial variability (Figure 4.6c). Over the western and southern parts of the country, there are weak positive anomalies, while the central to northeastern parts have weak negative anomalies. Specifically in the eastern escarpment study site, weak positive anomalies are present during Neutral events (Figure 4.6c).

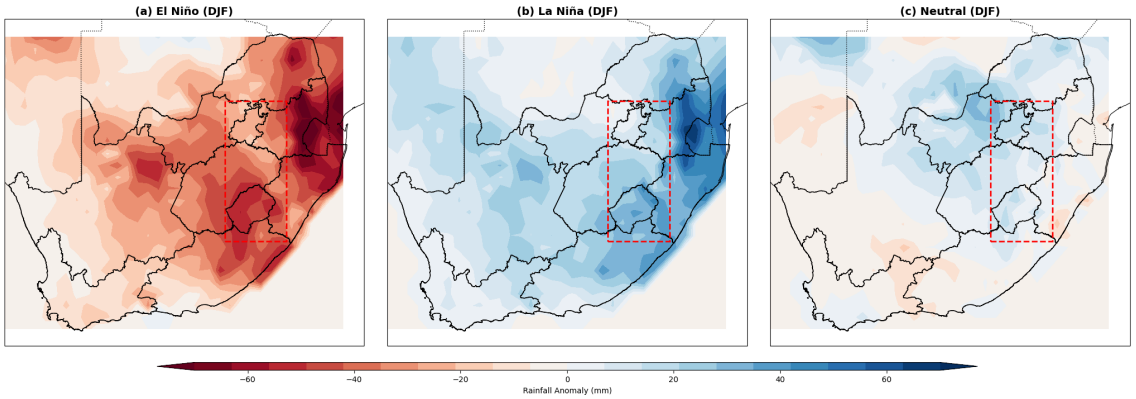

Figure 4.6: Rainfall anomaly maps (mm) for DJF, associated with the ENSO cycle based on ENSO events between 1981 and 2023, for (a) El Niño, (b) La Niña and (c) Neural phases. Anomalies are calculated from the 1981-2023 average.

The rainfall anomaly plot for MAM shows a similar but substantially weaker ENSO signal compared to DJF. That is, overall, below-normal conditions occur during El Niño and above-normal conditions during La Niña, but the amplitude of the anomalies are much weaker (Figure 4.7). These results show that ENSO maintains its effect into the MAM season, but there is a clear weakening of the signal. Over the eastern escarpment study site, generally below-normal (above-normal) conditions occur during El Niño (La Niña), although anomalies are weak (Figure 4.7a,b). It is notable that the amplitude of anomalies during the Neutral phase is similar to El Niño/La Niña phases. Over the eastern escarpment study site, Neutral phases are associated with weak positive anomalies in the northern parts and weak negative anomalies in the southern parts (Figure 4.7c).

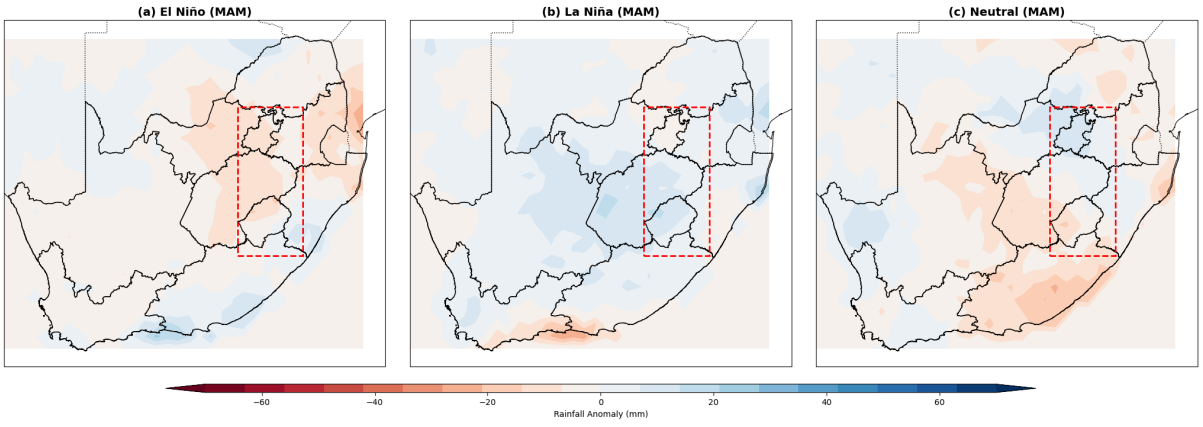

Figure 4.7: Rainfall anomaly maps (mm) for MAM, associated with the ENSO cycle based on ENSO events between 1981 and 2023, for (a) El Niño, (b) La Niña and (c) Neural phases. Anomalies are calculated from the 1981-2023 average.

It is interesting to note that CRU shows a 'reversal' of the ENSO signal across southern Africa during JJA (Figure 4.8). That is, JJA seasons during El Niño years are associated with above-normal rainfall and during La Niña years are associated with below-normal rainfall. However, the low amplitude of these anomalies suggests a very weak signal (Figure 4.8a,b). Since JJA is not a primary rainfall season for much of South Africa (except the winter-rainfall zone in the southwestern Cape), the drying effect during El Niño years is not as pronounced as in DJF or SON. This weak signal is also present over the eastern escarpment study site, reinforcing the idea that ENSO does not necessarily reduce or enhance winter rainfall in this region. During Neutral years, there is spatial variability in the JJA rainfall anomalies, although most of southern Africa shows weak positive anomalies with some negative anomalies over KwaZulu Natal. Over the eastern escarpment study site, JJA seasons during Neutral years show predominantly weak positive anomalies (Figure 4.8c).

During El Niño years, most of southern Africa is drier than normal during SON seasons, with more pronounced drying shown over northeastern South Africa (Figure 4.9a). Over the eastern escarpment study site, there is a mixed signal for SON seasons during El Niño years. That is, the northern parts of the study site show drying and the southern parts show wetting (Figure 4.9a). As with DJF, wet conditions during La Niña years are present in the SON season, although the amplitude is weaker. Over the eastern escarpment study site, SON seasons during La Niña years show above-normal rainfall throughout the domain (Figure 4.9b). During Neutral years, Neutral SONs are associated with wetter conditions in the southwestern and northeastern parts, and drier conditions over northern, central and eastern parts of the country (Figure 4.9c). Over the eastern escarpment, most of the area receives below-normal rainfall during Neutral years, with a small region in the north getting above-normal rainfall (Figure 4.9c).

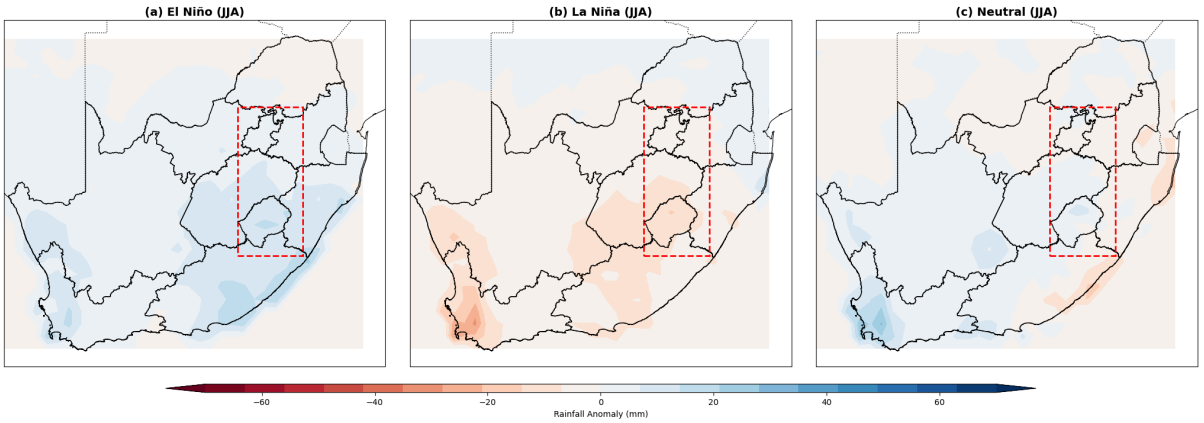

Figure 4.8: Rainfall anomaly maps (mm) for JJA, associated with the ENSO cycle based on ENSO events between 1981 and 2023, for (a) El Niño, (b) La Niña and (c) Neural phases. Anomalies are calculated from the 1981-2023 average.

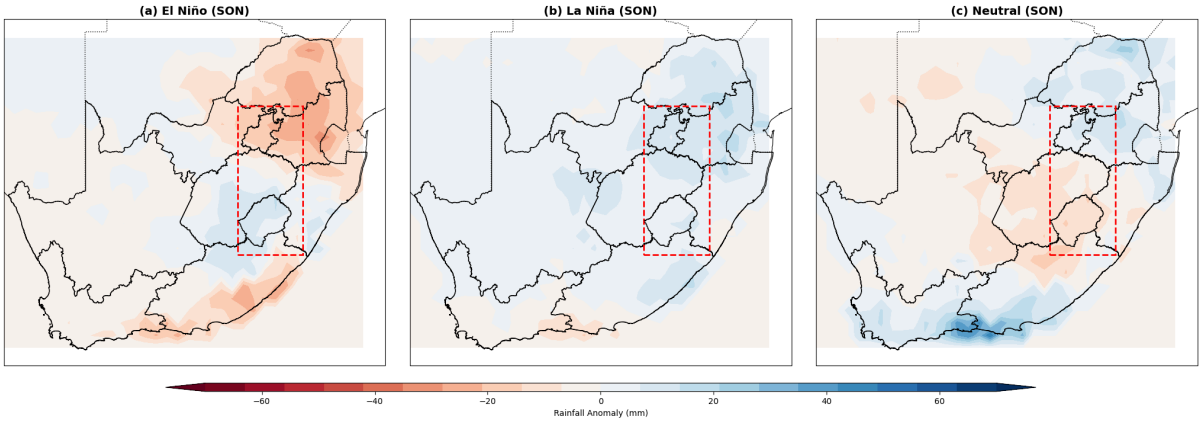

Figure 4.9: Rainfall anomaly maps (mm) for SON, associated with the ENSO cycle based on ENSO events between 1981 and 2023, for (a) El Niño, (b) La Niña and (c) Neural phases. Anomalies are calculated from the 1981-2023 average.

Chapter 5: ERA5 Data Validation

Chapter 5 focuses on the analysis of rainfall distribution across South Africa, with a focus on the eastern escarpment study site, using ERA5 reanalysis data. This chapter aims to investigate how well the reanalysis data set compares to the CRU observations in terms of different rainfall characteristics, including the representation of the ENSO-rainfall teleconnection to the region.

5.1 ERA5 Rainfall Distribution and Variability

The ERA5 dataset, known for its assimilation of multiple meteorological inputs and high-resolution reanalysis, presents a detailed picture of the spatial distribution of rainfall across the country and study site. The ERA5 data set correctly captures the well-known west-east rainfall gradient across the country (Figure 5.1). That is, rainfall totals are lowest in the western extent of South Africa, gradually increasing towards the eastern extent of South Africa, as is evident in the CRU observations (Figure 5.1b). Within the eastern escarpment study site, mean annual rainfall is lowest in the northern parts (600-650 mm) and highest along the Lesotho border in the southeastern parts (over 1200 mm) (Figure 5.2a, red box). The CRU observations display a similar north-south gradient within the study site. While the spatial distribution of rainfall of the country is similar to observations, it is clear the magnitude of annual mean rainfall in ERA5 is much higher (Figure 5.1).

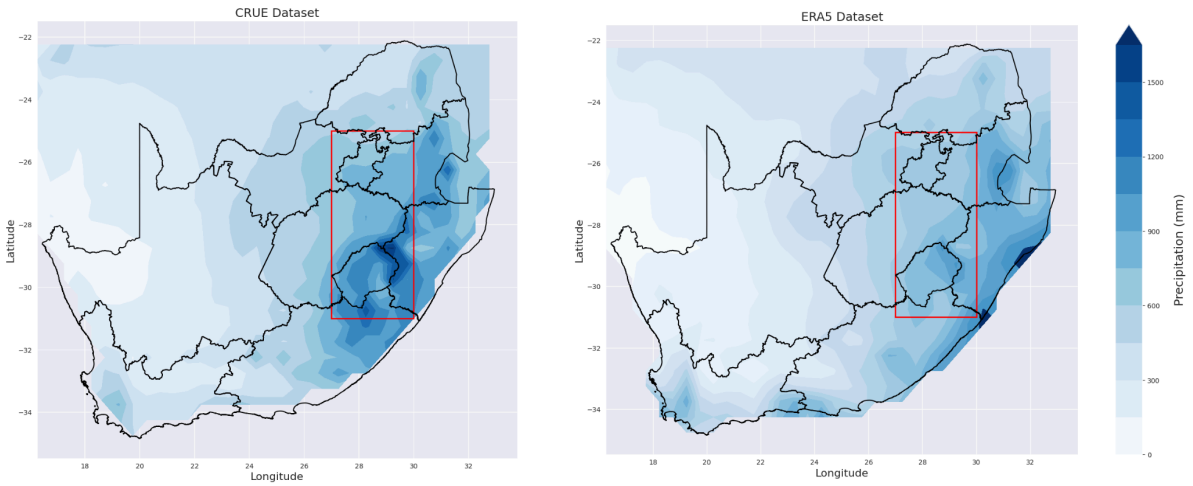

Figure 5.1: Spatial distribution in seasonal mean annual rainfall in the (a) ERA5 and (b) CRU data sets, for the period 1981-2023. The red box highlights the eastern escarpment study site.

The seasonal rainfall totals as estimated from the ERA5 are presented in Figure 5.2. There is a very strong seasonality over the area which is mainly due to the north-south movement of the Intertropical Convergence Zone (ITCZ) during the year (Jones and Carvalho, 2002). This is also well captured by the ERA5 reanalysis data and the rainfall is highest during the austral summer and spring months and lowest during the autumn and winter (Figure 5.2). On average across South Africa, precipitation is highest during the DJF season (170.98 mm), followed by the SON season (89.51 mm), the MAM season (85.53 mm) and the JJA season (28.81 mm) as presented in Table 5.1.

The ERA5 data shows that the rainfall signal is greatest during the DJF in the eastern escarpment study area with an average of 420.24 mm, a minimum of 59.94 mm and a maximum of 1373.59 mm (Table 5.2). The variability is also large with a standard deviation of 164.43 mm. The IQR is 308.74 to 498.63 mm (25th to 75th percentiles) which shows that there is very high rainfall and significant spatial variability of the rainfall in the region during this period. These values support and agree with the observed values from CRU that the DJF is the wettest season in the escarpment and the country as a whole.

Rainfall during the MAM period is among the lowest across both South Africa and the eastern escarpment. The national average decreases to 85.53 mm with a maximum of 816.80 mm and a standard deviation of 78.93 mm (Table 5.1). This seasonal decline is captured more distinctly by the ERA5 reanalysis data particularly in the eastern escarpment where rainfall is reduced to 182.24 mm on average (Table 5.2). Variability also decreases with a standard deviation of 82.80 mm. This shows a more defined and predictable rainfall pattern during the post-summer transition season, in line with the overall climatological tendencies of the country.

JJA remains the driest season in South Africa, and according to the ERA5 data set, the average rainfall across the country is 28.81 mm, the highest monthly total is 514.27 mm, and the standard deviation is 43.37 mm (Table 5.1). The rainfall in the eastern escarpment is just 49.51 mm on average, with a maximum of 254.08 mm and has the lowest variability among the seasons (standard deviation 39.69 mm, Table 5.2). The interquartile range of 18.20-71.26 mm suggests low seasonal activity, as expected for this dry period, and is consistent with the CRU observations. During SON, rainfall increases again in both country-wide averages and the study site. According to ERA5, the rainfall across South Africa is 89.51 mm with standard deviation of 100.92 mm and the highest rainfall of 879.20

mm (Table 5.1). The eastern escarpment also experiences a significant increase with an average of 249.91 mm and a high standard deviation of 113.19 mm (Table 5.2). This aligns with observations that SON is the second wettest season.. In general, ERA5 reproduces the spatial and seasonal precipitation patterns over South Africa and the eastern escarpment in conformity with the CRU-based climatologies.

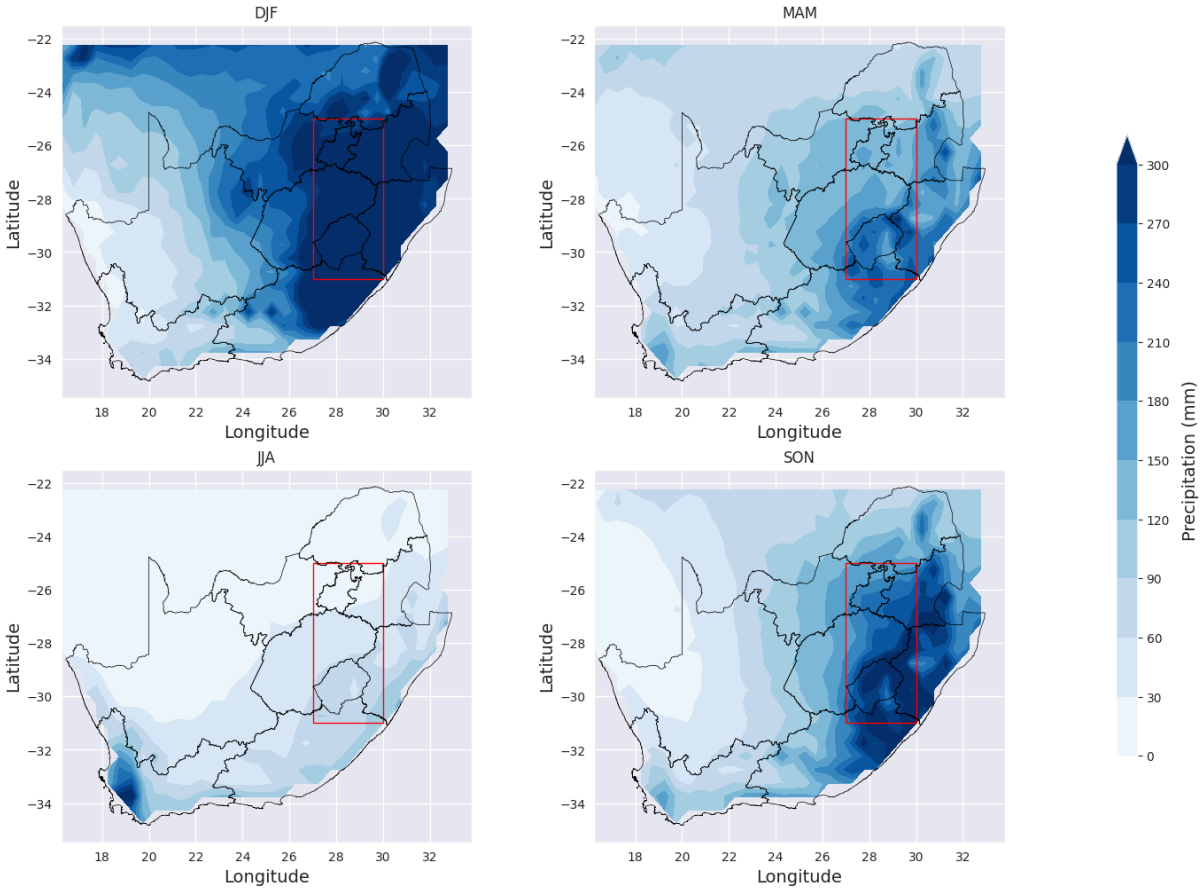

Figure 5.2: Mean seasonal ERA5 rainfall totals (mm) across South Africa for 1981-2023, with the rectangular (red) box highlighting the study site.

Table 5.1: Rainfall statistics per season across South Africa for the period 1981-2023

Season	Mean	Minimum	Maximum	Standard Deviation	25th Percentile	Median	75th Percentile
DJF	170.98	0	1373.59	167.27	24.13	132.7	268.21
MAM	85.53	0	816.8	78.93	21.24	69.94	128.75
JJA	28.81	0	514.27	43.37	0.48	11.26	40.74
SON	89.51	0	879.2	100.92	8.85	58.15	131.86

Table 5.2: Rainfall statistics per season across eastern escarpment study site, for the period 1981-2023

Season	Mean	Minimum	Maximum	Standard Deviation	25th Percentile	Median	75th Percentile
DJF	420.24	59.94	1373.59	164.43	308.74	389.96	498.63
MAM	182.24	12.58	624.34	82.8	121.85	170.64	232.76
JJA	49.51	0	254.08	39.69	18.2	40.45	71.26
SON	249.91	20.24	879.2	113.19	167.78	235.88	316.88

Figure 5.3 shows the mean annual rainfall distribution for CRU and ERA5 for the eastern escarpment study site. The distributions are remarkably similar, both showing a right skew distribution.. With a mean of 706.75 mm and a standard deviation of ±156.37 mm, the CRU dataset indicates that rainfall varies significantly. ERA5 is more variable in the annual total precipitation with a slightly higher mean value of 909.13 mm and even higher standard deviation of ±297.1 mm. This indicates a larger spread in the mean annual values recorded for ERA5. The tail of the ERA5 data set is wider compared to that of the CRU data set, suggesting that larger precipitation values are more frequent in ERA5. The lower density in the ERA5 plot suggests precipitation values are less frequently concentrated around the mean, reinforcing the higher variability noted in this data set. The shape of the ERA5 distribution plot shows a more significant right skew, which points to a higher occurrence of years with substantial rainfall, possibly capturing heavy rainfall events that might not be as

evident in the CRU data set. This could be due to ERA5's higher resolution and data assimilation techniques, which allow for more detailed and varied climatic data inputs.

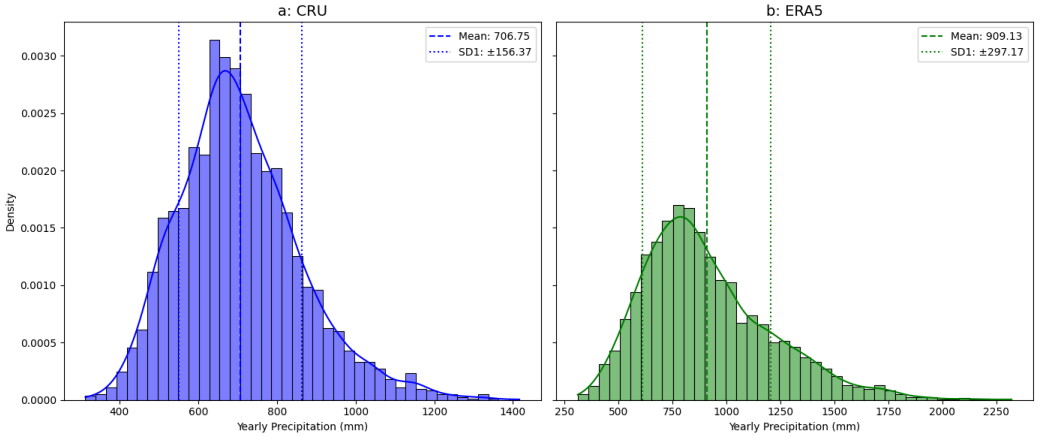

Figure 5.3: Mean annual rainfall distribution across the eastern escarpment study site for (a) CRU and (b) ERA5, with mean (thicker dotted line) and standard deviations (thinner dotted lines).

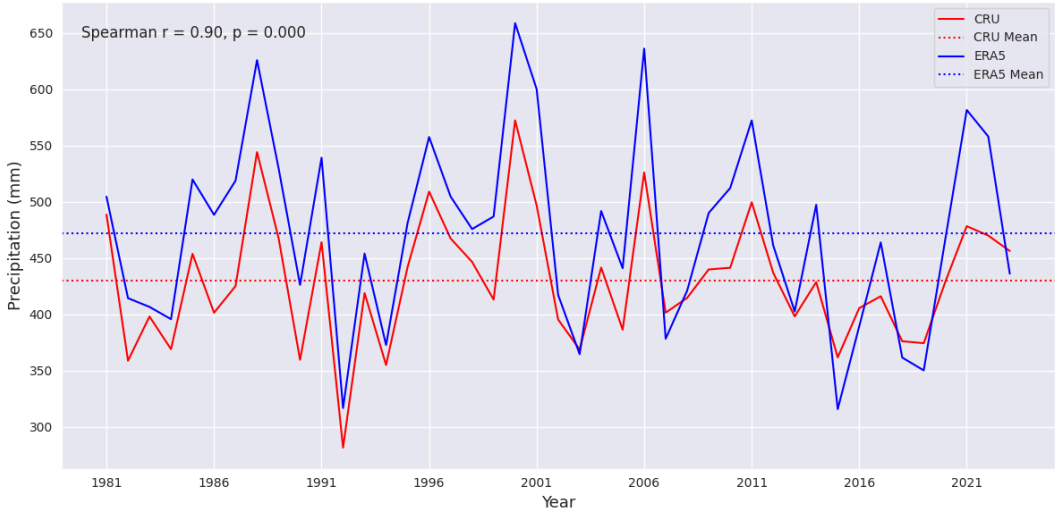

Figure 5.4: Interannual rainfall variability in the CRU (red line) and ERA5 (blue line) data sets, across the eastern escarpment study site, for the period 1981 to 2023.

Figure 5.4 displays interannual variability in both the CRU and ERA5 data for the eastern escarpment study region for the 1981-2023 period. There is a remarkable agreement in the trend between the two data sets, supported by the high spearman rank correlation (r = 0.9),

with cohesion in years that are wetter/drier. Nonetheless, ERA5 still depicts greater rainfall totals compared to CRU, as indicated by its higher mean precipitation (blue dotted line) compared to CRU (red dotted line). As previously illustrated, this result aligns with the expectation that ERA5, being of finer spatial resolution and having satellite assimilation, is able to realistically replicate the effect of localized precipitation features attenuated by CRU's station-based interpolation. Overall, ERA5 presents more intense precipitation peaks for extreme wet events, especially in 1999 and 2000. Nevertheless, it also reflects cases of rainfall underestimation with respect to CRU, for example in 2015 and 2018. Having said this, overall the peaks and troughs in the two datasets are well-aligned.

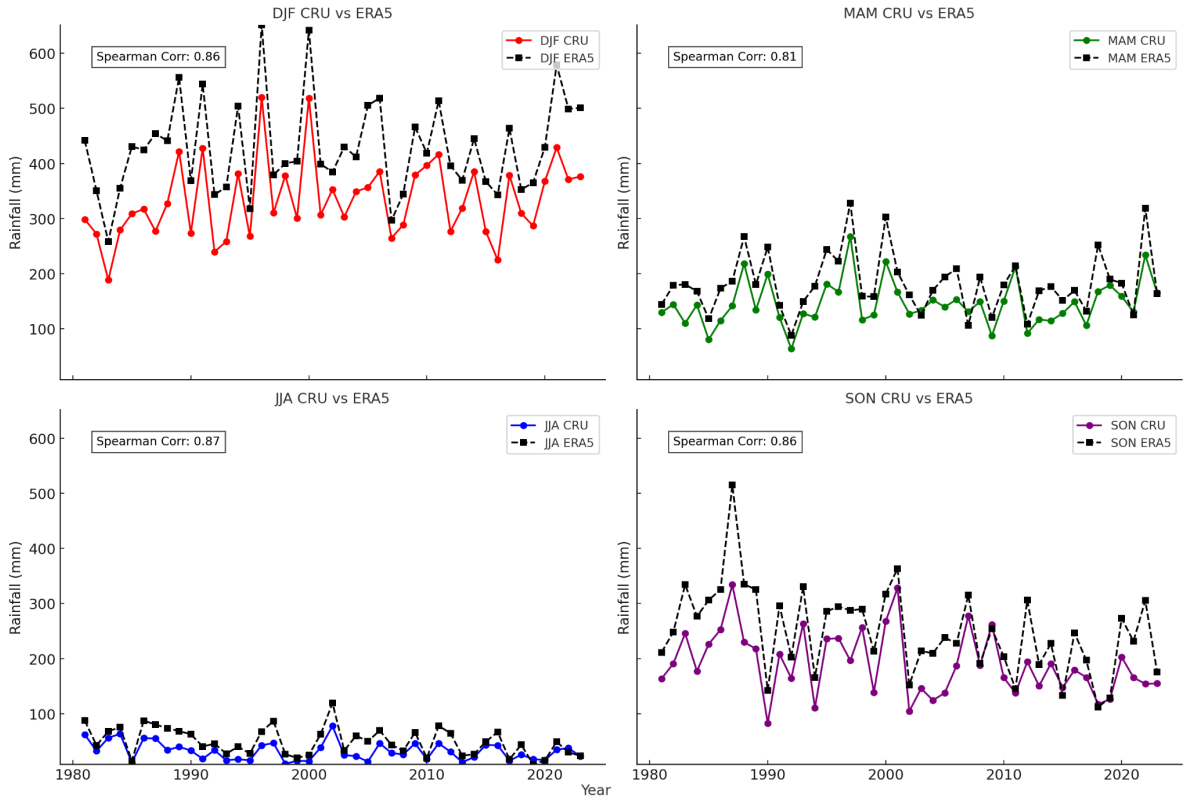

Figure 5.5: Interannual seasonal rainfall variability for CRU (solid coloured lines) and ERA5 (black dotted lines) across the eastern escarpment study site. Each subplot represents a different season (DJF, MAM, JJA, SON), and Spearman correlation coefficients indicate the similarity in rainfall variability between the two datasets for each season.

Seasonally, there is again remarkable agreement in the wetter and drier seasons across the two data sets and there is a strong correlation in all four seasons, with Spearman Rank correlation between 0.81 and 0.87 (Figure 5.5). This indicates that both data sets exhibit similar interannual rainfall variation, with some differences in the magnitude. The strongest

correlations are noted in the wet seasons of DJF (0.86) and SON (0.86). The persistent seasonality of these correlations supports the credibility of ERA5 in capturing observed rainfall behaviour from CRU. However, there is a consistent over-estimation in ERA5, across all four seasons, but it is most pronounced during DJF and then SON (Figure 5.5). MAM records the weakest correlation (0.81), suggesting the ERA5 reanalysis is slightly less skillful during this drier season. It is interesting that the correlation is marginally higher in JJA, despite this being the driest season in the region.

5.2 ERA5 Spatial Rainfall Biases

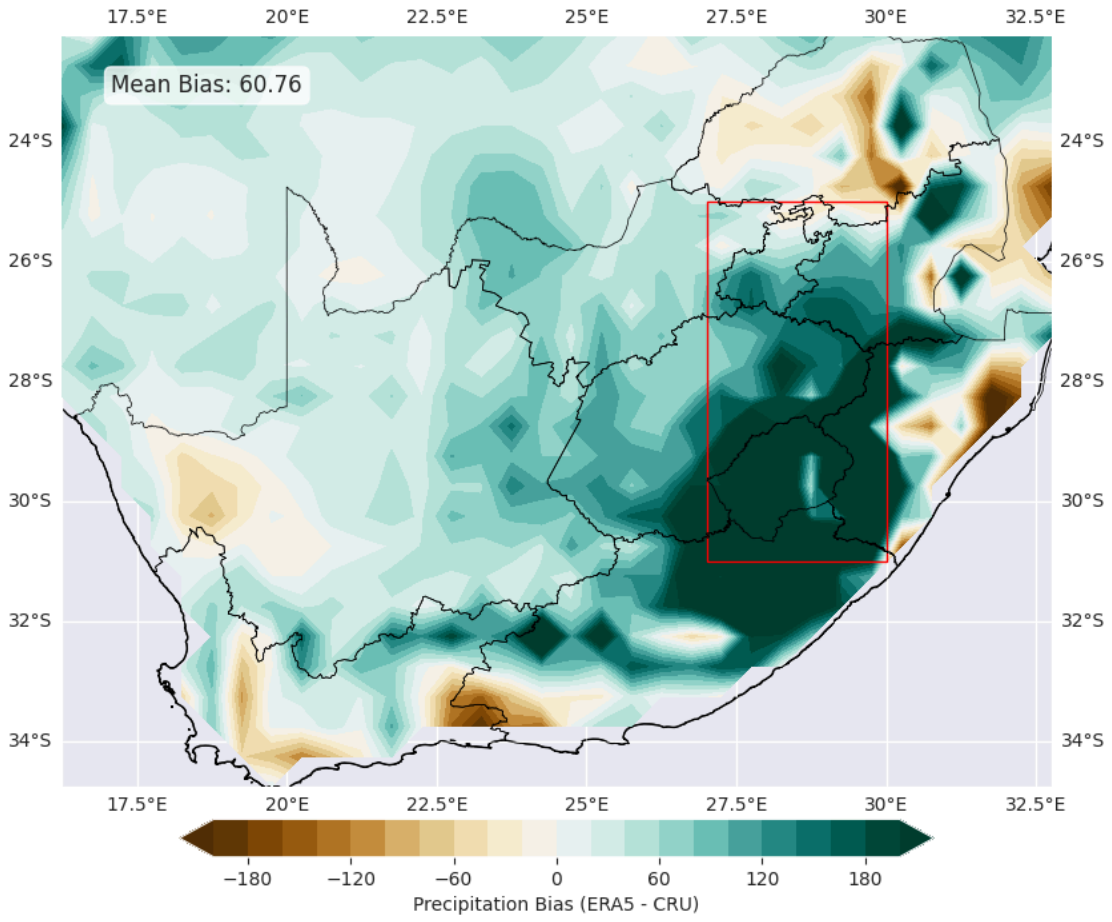

Figure 5.6: Mean annual rainfall bias (mm) in the ERA5 data relative to CRU.

Figure 5.6 is a spatial plot of the mean annual rainfall bias in ERA5 relative to CRU. Generally, ERA5 overestimates total annual rainfall across South Africa, with substantial biases in the eastern and southeastern parts of the country. In contrast, there are small areas in South Africa where ERA5 is underestimating the level of rainfall compared to CRU,

especially in the mountainous regions of the Western and Eastern Capes, as well as the northeastern coastal part of KwaZulu Natal and parts of Limpopo (Figure 5.6). Over the eastern escarpment study site, there is a large wet bias, particularly in the southern half of the region (Figure 5.6). The area-averaged bias across the country is +60.76 mm/year compared to 217.05 mm/year for the eastern escarpment study site, showing the substantial wet bias in that part of the country. These discrepancies may result from differences in data resolution and methodologies between the two datasets, but topography is also a likely factor, particularly over the Eastern Escarpment, where steep terrain enhances orographic precipitation (Taylor et al., 2016). ERA5 may overestimate rainfall in these areas due to its physical modeling of uplift and cloud processes, while CRU tends to underestimate rainfall due to sparse station coverage at higher elevations (Gleixner et al., 2020). This contrast is especially evident in the southern part of the study site, where ERA5 likely captures topography-driven rainfall more strongly, contributing to the observed wet bias (Taylor et al., 2016; Gleixner et al., 2020).

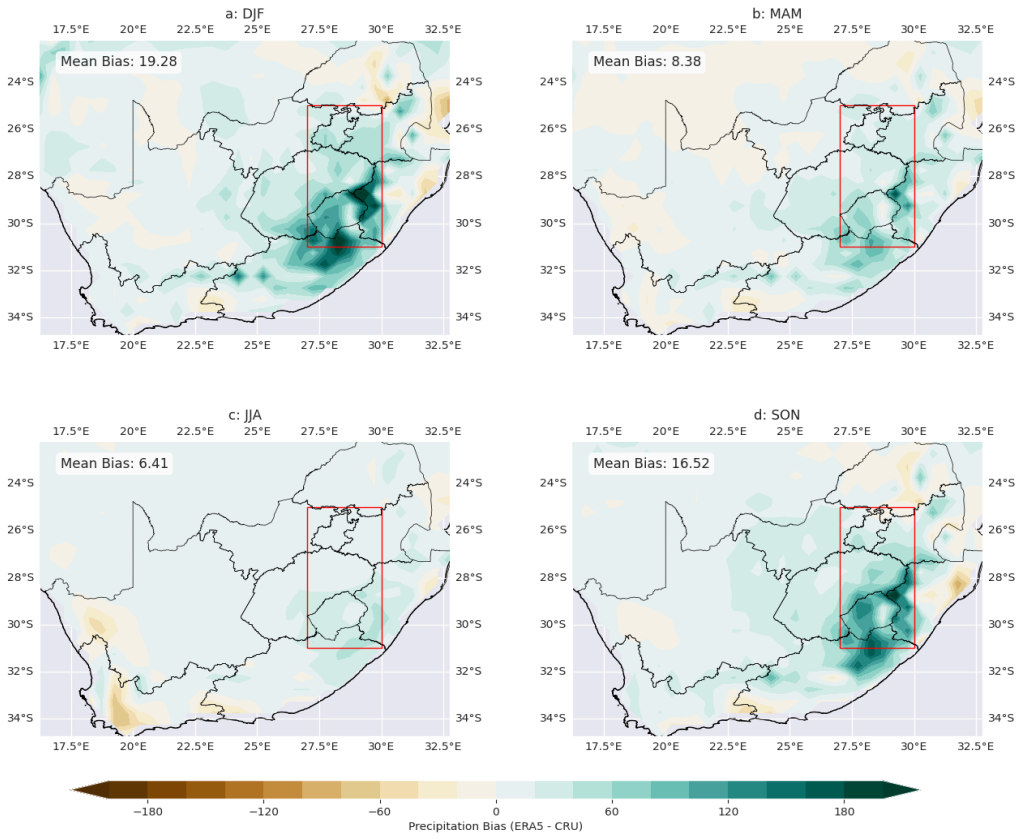

Figure 5.7: Seasonal bias in the ERA5 data relative to CRU for (a) DJF, (b) MAM, (c) JJA and (d) SON seasons.

The wet biases in the total annual rainfall are likely driven by the overestimation that is evident across all four seasons (Figure 5.7). Overall, the wet biases are larger in the summer and spring months and dry biases are larger in the winter and autumn months. During DJF, the largest wet biases are evident in eastern parts of South Africa, with substantial overestimations in the southern parts of the eastern escarpment study site (Figure 5.7a). During autumn (MAM), ERA5 continues to predominantly overestimate rainfall, especially over the eastern escarpment study site, but the biases are reduced in magnitude (Figure 5.7b). During the JJA season, which covers the winter months that are typically dry, the smallest mean bias is observed over the country and the study site (Figure 5.7c). It is interesting to note the larger dry biases over the Cape Fold Mountains in the Western Cape during JJA, which is a winter rainfall region and therefore ERA5 is underestimating totals in the peak rainfall season. During spring (SON), there is again a general overestimation in rainfall across the country, particularly over southern parts of the eastern escarpment study site, although not to the same magnitude as during DJF (Figure 5.7d). Understanding such biases in the annual and seasonal rainfall totals has significant implications for climatological investigation and application, particularly in the eastern escarpment study site, where topographic influence can potentially amplify differences (Taylor et al., 2016).

5.3 Statistical Insights into ERA5 and CRU data

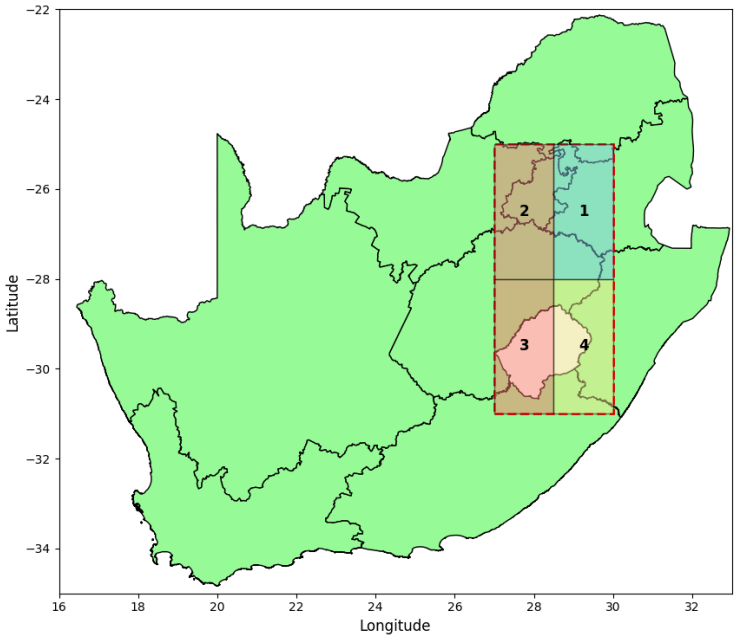

Figure 5.8: The four quadrants investigated within the eastern escarpment study site.

The analysis of the spatial distribution of precipitation in the eastern escarpment study site, illustrated in Table 5.3, shows clearly defined subregional and seasonal patterns for the four quadrants displayed in Figure 5.8. These quadrants were delineated to divide the study area into equal-sized subregions to enable comparative analysis across different parts of the escarpment. It is interesting to note that in both data sets, across all four quadrants, DJF has the highest rainfall totals, followed by SON, then MAM and JJA is the driest (Table 5.3), as is expected given the seasonal distribution of rainfall in the region. Notably, the northwestern region (quadrant 2) has lower precipitation totals compared to the rest of the regions, particularly in the JJA season, where it has the lowest seasonal means of 8.97 mm in the CRU data set and 15.01 mm in the ERA5 data set. In contrast, the southeastern region receives large amounts of rainfall, and the highest DJF mean precipitation values (359.94 mm in CRU and 486.96 mm in ERA5). This is consistent with the observed north-south gradient in the mean annual rainfall totals, and is likely driven by the influence of the Indian Ocean moist air, which is forced to interact with the orographic characteristics of the eastern escarpment, resulting in increased orographic and convective rainfall in the southern parts of the region (Taylor et al., 2016).

The orographic characteristics of the escarpment region influences spatial variability of rainfall and the performance of gridded datasets. The accuracy of CRU, which depends on interpolation from ground-based measurements, is influenced by the distribution and density of weather stations. According to Harris et al. (2020), station coverage varies geographically and is lower in higher elevation and rural areas. In mountainous regions, this can result in less interpolation, which might lead to an underestimation of rainfall. On the other hand, ERA5 uses data assimilation to merge several data sources, which can enhance representation in areas with limited ground data (Gleixner et al., 2020).

In MAM rainfall decreases across all quadrants, marking the transition from peak summer rainfall to drier conditions. ERA5 consistently overestimates peak values with respect to CRU, especially in the southern parts of the region (quadrants 3 and 4), where convective rainfall is more common. For example, in the southwestern part (quadrant 3), CRU records a mean of 158.52 mm, whereas ERA5 records 194.47 mm, with a peak value of 476.13 mm, much greater than CRU's peak value of 390.1 mm. JJA is the driest season, especially in northwestern areas, with the northwestern region (quadrant 2) recording the lowest seasonal mean (8.97 mm in CRU, 15.01 mm in ERA5). Interestingly, the southern region (quadrants 3 and 4) receives slightly more precipitation, likely influenced by orographic rainfall and

frontal systems. During SON rainfall increases again, particularly in the southeastern region (quadrant 4), where ERA5 (294.1 mm) exceeds CRU (215.1 mm). This quadrant also records the highest maximum rainfall in both data sets, reflecting the early intensification of convective storms before DJF. In contrast, the northwestern region (quadrant 2) experiences a more gradual increase in rainfall, with ERA5 closely matching the observations (CRU = 123.53 mm, ERA5 = 129.34 mm). The seasonal variations and contrast in rainfall intensity from northwestern to southeastern regions highlights the influence of topography, atmospheric circulation, and proximity to moisture sources shaping rainfall patterns. The ability of ERA5 to correctly capture these spatial variations within a relatively small region, when compared to observations, underscores its usefulness for studying localized climate dynamics. However it is important to acknowledge that CRU, which serves as the observational reference for this study, is itself influenced by the availability of weather stations. Therefore, in areas with sparse station coverage, particularly in complex terrains, interpolation challenges may affect the accuracy of CRU.

Table 5.3: Statistical summary for seasonal rainfall for all quadrants in the eastern escarpment

Region	Season	CRU Mean	CRU Minimum	CRU Maximum	ERA5 Mean	ERA5 Minimum	ERA5 Maximum
Northeastern Escarpment (1)	DJF	271.98	44.2	652.8	269.56	46.23	689.61
	MAM	96.97	3.8	280.4	99.27	4.37	351.33
	JJA	12.16	0	68.1	16.86	0	85.33
	SON	147.44	22.7	366.6	144.11	17.25	459.12
Northwestern Escarpment (2)	DJF	274.89	46.9	568	273.07	47.85	975.13
	MAM	97.22	6.7	332.8	102.33	5.87	360.55
	JJA	8.97	0	68.4	15.01	0	81.5
	SON	123.53	23.4	351.4	129.34	16.95	447.68
Southwestern Escarpment (3)	DJF	304.17	61.9	626.6	409.34	105.03	971.06
	MAM	158.52	39.1	390.1	194.47	42.34	476.13
	JJA	37.46	0.1	154.8	57.61	0.06	212.76
	SON	174.66	18.6	408.3	246.14	20.24	692.42
Southeastern Escarpment (4)	DJF	359.94	116	759	486.96	119.35	1373.59
	MAM	151.09	35.5	448.8	193.71	43.71	624.34
	JJA	38.25	1.3	137.9	60.39	0.6	254.08
	SON	215.1	61.8	526.3	294.1	68.98	879.2

5.4 Evaluating the ENSO-Rainfall Relationship in ERA5

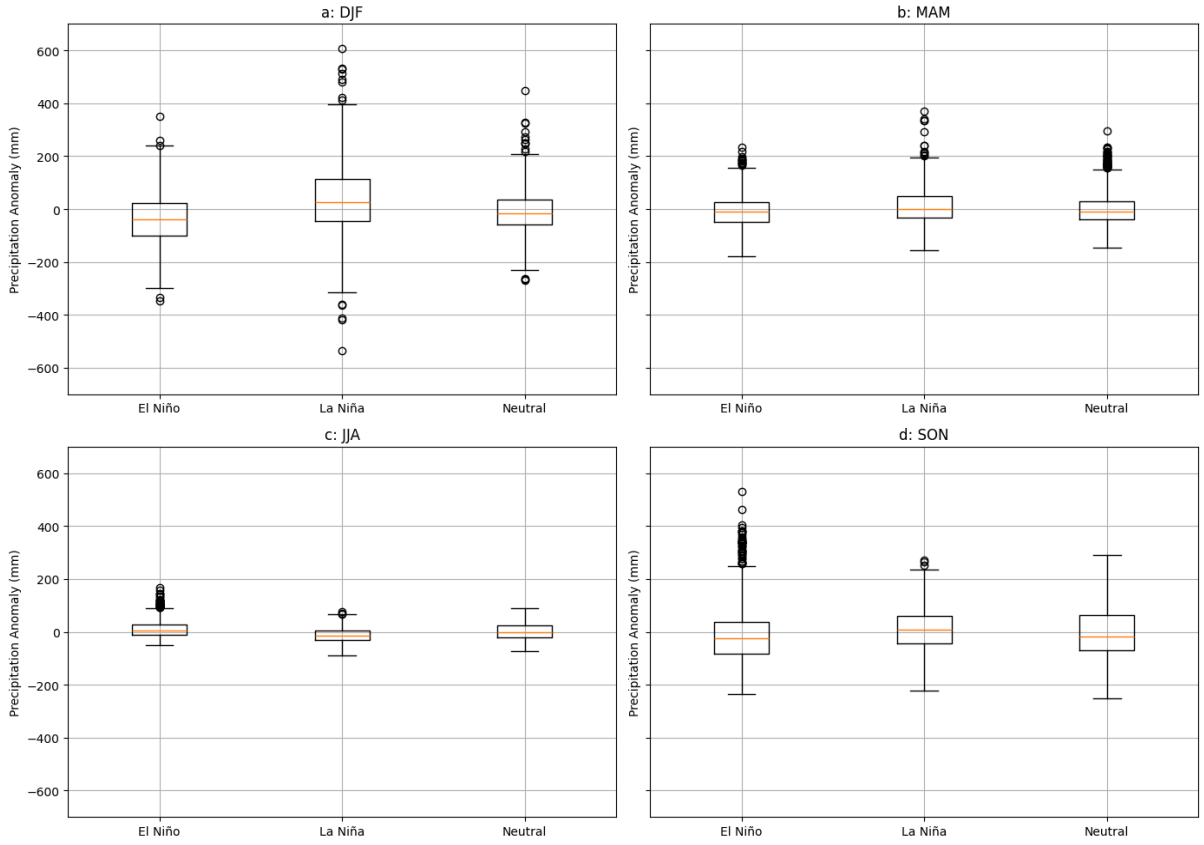

Figure 5.9: Spread in the seasonal rainfall anomalies according to specific ENSO phases, across the eastern escarpment study site, for (a) DJF, (b) MAM, (c) JJA and (d) SON. Boxplots show the 25th, 50th and 75th percentiles; whiskers extend to the most extreme values within 1.5 × IQR from the lower and upper quartiles; circles represent outliers beyond this range.

The distribution of the ERA5 rainfall anomalies at the grid level within the eastern escarpment study area is very similar to observations (see Chapter 4). The dry conditions that are prominent over the region during El Niño events and wet conditions during La Niña events are easily identifiable in the boxplots for the DJF and SON periods (Figure 5.9a and d). In all the seasons, ERA5 has a higher range of anomalies and is able to simulate more frequent extreme wet and dry conditions, especially in DJF and SON, the periods of highest ENSO influence. There are some grid boxes with positive anomalies in El Niño and negative anomalies in La Niña in all the seasons, but the median clearly shows that the

majority of grid boxes capture the classic ENSO–rainfall relationship of dry (wet) conditions in El Niño (La Niña). While the results compare well to CRU, the magnitude of the anomalies in ERA5 are larger. The anomalies are also less dispersed in MAM and JJA, which shows that the anomalies are generally smaller in these months (Figure 5.9b and c). There is also a smaller difference in the quantile values across different ENSO phases, suggesting the ENSO teleconnection to rainfall during these seasons is much weaker.

The shape of the boxplots also helps to support this distinction by season. DJF and SON have fairly wide interquartile ranges, and there are many outliers both in La Niña and El Niño conditions, which means that the response is highly variable across the eastern escarpment study site. Some anomalies in DJF are higher than +600 mm in La Niña and lower than –400 mm in El Niño. These patterns suggest that the ERA5 reanalysis dataset is capable of capturing the presence of extreme rainfall events. There is also a high variability in SON especially in the upper quartiles during La Niña and this is accompanied by many grid points having anomalies greater than +400 mm.

However, the anomaly distributions in MAM and JJA are more compact and the range between the 25th and 75th percentiles is narrower for all the ENSO phases. This further suggests that large-scale ENSO forcing has little impact during these seasons. In JJA, during the dry winter, rainfall anomalies are also very much constrained and most of the values are within ±100 mm irrespective of the ENSO phase. The low standard deviations and the lack of extreme outliers in both MAM and JJA further support this limited ENSO impact. However, it is important to acknowledge that this does not rule out the role of localised processes such as cut-off lows and pressure systems, which may contribute to rainfall extremes or suppress variability in ways that are not fully captured by the statistical approach used.

Table 5.4 shows the variable response in DJF rainfall to different ENSO events, which have been ranked according to the Niño 3.4 index. Overall, the ERA5 results align well with CRU and capture the well-known ENSO-rainfall teleconnection of dry conditions during El Niño events and wet conditions during La Niña events. It is notable that the 1982/3 El Niño was the driest event in the observations in terms of anomalies across both South Africa and the eastern escarpment study site and ERA5 is the same. It is interesting that the 1994/5 and 2006/7 events are significantly dry in the ERA5 data set, much drier than CRU, while ERA5 underestimates the magnitude of drying during the well-known 2015/6 event (Table 5.4).

However, the 1986/7 and 2002/3 events are exceptions, with drying persisting over the country, but positive anomalies present over the eastern escarpment study site (Table 5.4). Interestingly, above-normal rainfall for both South Africa and the eastern escarpment study site is recorded during the weak El Niño events of 1987/8 and 2004/5, similar to the observations.

Table 5.4: Ranking of El Niño and La Niña events across South Africa and the eastern escarpment study site, for the DJF season

Ranked El Niño Events	DJF Niño 3.4 index (El Niño)	DJF rainfall anomaly South Africa (El Niño)	DJF rainfall anomaly Eastern Escarpment (El Niño)	Ranked La Niña Events	DJF Niño 3.4 index (La Niña)	DJF rainfall anomaly South Africa (La Niña)	DJF rainfall anomaly Eastern Escarpment (La Niña)
2015/6	2.41	-52.73	-77.34	1988/9	-1.77	67.31	135.95
1982/3	2.33	-81.24	-161.97	2007/8	-1.7	-2.66	-75.66
1997/8	2.27	-25.83	-20.46	1999/0	-1.62	148.52	221.14
1991/2	1.62	-64.76	-76.71	2010/1	-1.53	77.26	93.5
2009/0	1.47	15.59	-1.75	1998/9	-1.48	0.86	-15.98
1986/7	1.11	-33.4	33.81	1983/4	-1.11	-3.65	10.46
1994/5	1.06	-60.77	-102.15	2017/8	-0.81	115.64	158.65
2002/3	1.01	-22.37	9.72	2005/6	-0.81	-21.93	-21.29
2018/9	0.7	-39.14	-55.03	2000/1	-0.81	78.67	98.3
1987/8	0.7	43.21	20.81	2008/9	-0.87	28.82	45.86
2014/5	0.64	-42.35	-53.08	2011/2	-0.86	-0.62	-24.34
2006/7	0.6	-61.67	-123.73	2021/2	-0.84	27.5	78.51
2004/5	0.51	6.12	85.01	2022/3	-0.75	-105.87	-238.51

As expected, the La Niña events are generally associated with above-average rainfall, particularly in the eastern escarpment, although there is greater variability in the rainfall response, as was noted in the observations (see Chapter 4). Observations from the CRU data set indicate that the 1988/89 and 1999/2000 La Niña events produced the most significant positive rainfall anomalies across South Africa, with substantial positive anomalies over the eastern escarpment study site. ERA5 also captures this result, with stronger anomalies over the eastern escarpment study site (1988/9 = 135.95 mm, 1999/2000 = 221.14 mm) than South Africa (1988/9 = 67.31mm, 1999/2000 = 148.52mm). However, there are some La Niña events associated with negative rainfall anomalies (e.g. 2007/8, 2005/6 and 2022/3), as was also evident in the observations. The 2022/3 La Niña stands out as an extreme case, with a strong drying signal (-105.87 mm across South Africa and -238.51 mm over the eastern escarpment study site). Overall, as with the observations, the magnitude of ENSO's impact on the eastern escarpment is larger than the country-wide average. The interannual variability (in terms of variable rainfall responses to different ENSO events) noted in the observations is evident in ERA5.

5.5 Representation of the ENSO signal in ERA5

This section presents ERA5 seasonal composite rainfall anomaly plots of the various ENSO events that occurred between 1981 and 2023 (Figures 5.10–5.13). This investigation provides insights into how well the ERA5 reanalysis data captures the ENSO-rainfall signal over the region. During DJF, below-normal rainfall conditions occur over the country during El Niño events, with severe drying over most of the eastern escarpment study site (Figure 5.10). This closely resembles the CRU-based DJF composite (Chapter 4, Figure 4.7), which also depicts below-normal rainfall during El Niño over southern Africa, but the magnitude of the anomalies is larger in ERA5 (Figure 5.10). As with the observations, stronger drying occurs over eastern parts of the country, compared to the western parts, during El Niño events. Over the eastern escarpment study site, dry conditions occur over most of the region during El Niño events, with a small subregion in the east recording very weak anomalies (Figure 5.11a). There is a clear wet signal during La Niña events (Figure 5.11b). These anomalies closely resemble observations, but with larger magnitudes in parts of the country. The above-normal rainfall conditions during La Niña events are well captured in ERA5 over the eastern escarpment study site. Neutral phases show similar spatial patterns to

observations, with negative anomalies over the western and eastern parts and positive anomalies over the central parts of the country.

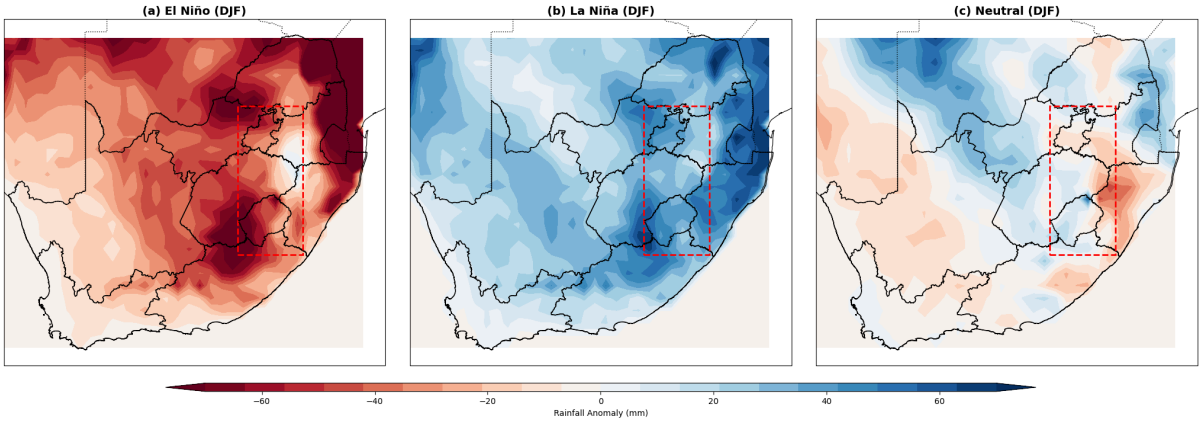

Figure 5.10: Rainfall anomaly maps (mm) for DJF, associated with the ENSO cycle based on ENSO events between 1981 and 2023, for (a) El Niño, (b) La Niña and (c) Neural phases. Anomalies are calculated from the 1981-2023 average.

The composite anomaly plots for MAM (Figure 5.11) illustrate that ENSO effects persist into autumn, though with some reduction in magnitude compared to summer. Overall, both ERA5 and CRU show that El Niño years continue to be drier and La Niña years wetter than average in MAM. However, the influence of ENSO during MAM appears somewhat moderate compared to the peak summer season. As with DJF, the amplitude of anomalies is slightly larger in ERA5 when compared to CRU. In ERA5, during MAM, much of the eastern and central escarpment exhibits significant negative anomalies, extending the El Niño induced dryness over a broad area. ERA5 does well at capturing the observed El Niño-induced drying signal over the eastern escarpment study site during MAM (Figure 5.11a), consistent with previous findings on its improved performance in simulating seasonal precipitation over southern Africa (Gleixner et al., 2020). Furthermore, the positive anomalies that occur during La Niña events over the country as a whole and the eastern escarpment study site (Figure 5.11b), are also consistent with observations. Neutral phases show a different spatial pattern in anomalies during MAM compared to DJF, consistent with observations. Specifically, over the eastern escarpment study site most of the region experiences wetter conditions, while southern parts experience drier conditions (Figure 5.11c).

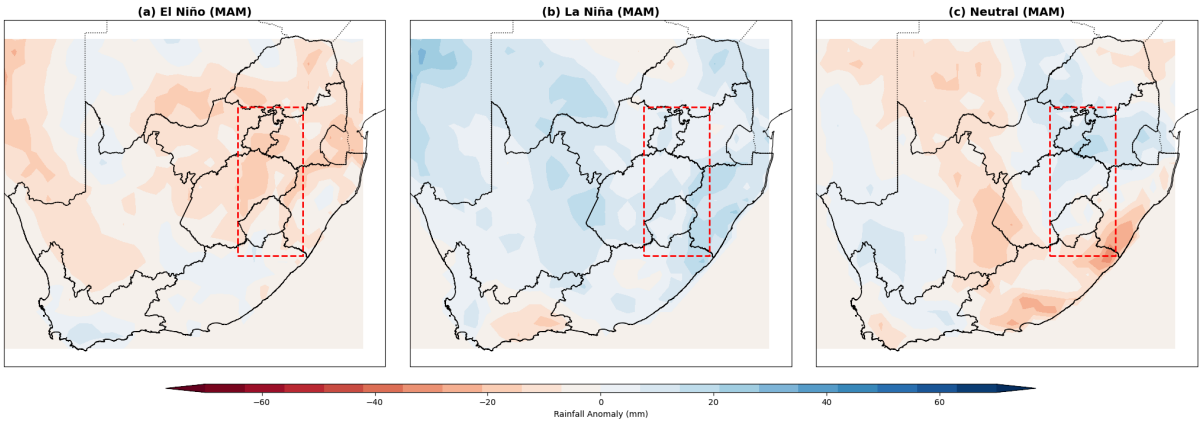

Figure 5.11: Rainfall anomaly maps (mm) for MAM, associated with the ENSO cycle based on ENSO events between 1981 and 2023, for (a) El Niño, (b) La Niña and (c) Neural phases. Anomalies are calculated from the 1981-2023 average.

It is interesting that JJA seasons during El Niño years are associated with positive rainfall anomalies over most of South Africa, with the exception being negative anomalies over the Limpopo Province (Figure 5.12a). Furthermore, JJA seasons during La Niña years are associated with negative anomalies over most of the country (Figure 5.12b). This means ERA5 displays above-average (below-average) winter rain in most of the country during El Niño (La Niña) years, contrary to the expected El Niño (La Niña) effect of drying (wetting). The 'reversal' of the rainfall anomalies associated with each phase of ENSO when compared to other seasons, is also notable in the CRU observations (see Chapter 4). The eastern escarpment study site shows the same response to ENSO during JJA, with wetter conditions present during El Niño and drier conditions during La Niña's (Figure 5.12). This aligns with observations and suggests that winter rainfall in this region is not necessarily enhanced or reduced by ENSO. During neutral years, most of the country experiences slightly wetter conditions during JJA, with some drying over parts of KwaZulu Natal and the Eastern Cape (Figure 5.12c). This spatial pattern in the anomalies is the same as observations.

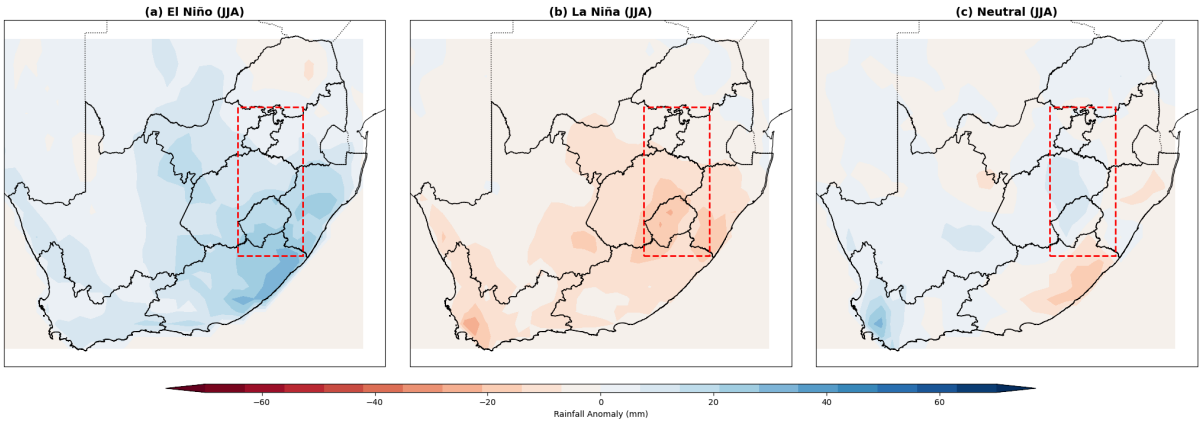

Figure 5.12: Rainfall anomaly maps (mm) for JJA, associated with the ENSO cycle based on ENSO events between 1981 and 2023, for (a) El Niño, (b) La Niña and (c) Neural phases. Anomalies are calculated from the 1981-2023 average.

The SON season marks the onset of the summer rains in the eastern parts of South Africa, and there are usually dry conditions during El Niño and wet conditions during La Niña (See Chapter 4). Broadly, ERA5 captures the same ENSO-driven rainfall anomalies (Figure 5.13). During El Niño events in SON, most of the country is drier than normal, with pronounced drying over the northeastern parts of the country (Figure 5.13a). Over the eastern escarpment study site, there is a mixed rainfall response. Specifically, drier conditions are present for the central to northern parts, while the southern parts show wetter conditions. A similar pattern was observed in CRU, but with the wetter conditions in the south spreading further north (see Chapter 4). It is interesting to note that where the ENSO signal in the SON rainfall is strong in the observations, ERA5 also shows anomalies of stronger magnitude. La Niña springs exhibit a clear wet signal in both ERA5 and CRU data sets. ERA5 depicts a widespread increase in precipitation during SON seasons of La Niña years, with strong positive anomalies covering most of South Africa (Figure 5.13b). Over the eastern escarpment study site, wetter-than-normal conditions occur for SON rainfall during La Niña years. During neutral ENSO springs, there is much spatial variability in the rainfall anomaly patterns across the country. Similar to observations, SON is associated with wetter conditions in the southwestern and northeastern parts, and drier conditions over northern, central and eastern parts of the country (Figure 5.13c).

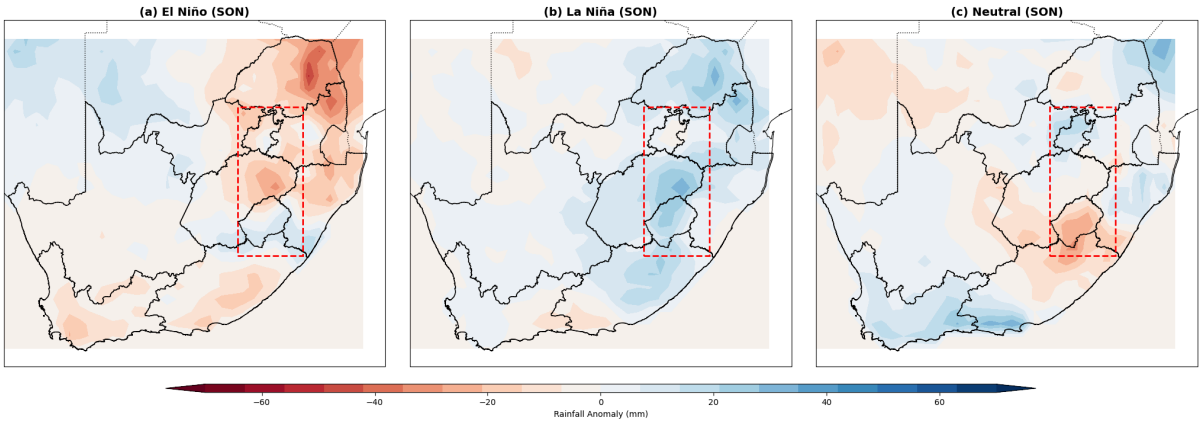

Figure 5.13: Rainfall anomaly maps (mm) for SON, associated with the ENSO cycle based on ENSO events between 1981 and 2023, for (a) El Niño, (b) La Niña and (c) Neural phases. Anomalies are calculated from the 1981-2023 average.

Across all seasons (DJF, MAM, JJA, SON), the ERA5 reanalysis data show a high degree of consistency with the CRU observational data set in capturing the influence of ENSO on South African rainfall. This comparative analysis demonstrates that ERA5 rainfall fields are good approximations of observations. Furthermore, the ERA5 and CRU comparison provides insight into how data characteristics influence the depiction of rainfall anomalies. ERA5 uses more detailed data and a higher-resolution model, which helps it show sharper differences in rainfall. This makes extreme wet and dry areas stand out more clearly compared to what is shown in the CRU dataset.These differences observed consistently suggest that ERA5 can capture fine-scale events that the CRU data may under represent. This complementary use of reanalysis and observational data provides a more comprehensive understanding of how El Niño, La Niña, and neutral conditions modulate seasonal rainfall over South Africa, and particularly the eastern escarpment study site.

Chapter 6: Discussion

6.1 Introduction

The overall objective of this study is to examine the characteristics of rainfall in South Africa with a specific focus on the eastern escarpment and to determine the influence of ENSO events on rainfall in the region. Since rainfall variability plays a crucial role in shaping hydrological resources and water security, this study is important for understanding how ENSO influences rainfall patterns affecting the eastern escarpment, a key water source for southern Africa. This chapter will discuss the results of this study in relation to previously completed studies. The chapter is structured as follows, the first section reflects on the rainfall distribution patterns in CRU and ERA5. The second section discusses the relationship between ENSO phases and rainfall anomalies. The third section explores regional disparities in ENSO's impact. The final section examines the implications of these findings for climate research, water resource management, and ENSO forecasting applications.

6.2 Comparison between CRU and ERA5 Rainfall Distributions

The rainfall distribution in South Africa is quite complex and shows a clear west-east gradient, with notably higher totals in the eastern parts of the country (Crétat et al., 2010), including the eastern escarpment. In Chapters 4 and 5, CRU and ERA5 datasets were used to investigate rainfall distribution, seasonality and the role of ENSO in rainfall variability. Both datasets capture the well-known west-east rainfall gradient across South Africa, with higher annual totals in the eastern escarpment region. However, ERA5 overestimates rainfall in the higher precipitation zones, in the eastern parts of the country, while it underestimates rainfall in parts of the lower rainfall zones in the west of the Northern Cape, and along the Cape Fold Mountains. The wet biases have been previously noted by Taylor et al. (2016) who established that the ERA5 dataset overestimates precipitation amounts in mountainous regions because of orographic influences. Furthermore, within the eastern escarpment study site, mean annual rainfall has a north-south rainfall gradient, and ERA5 notably overestimates rainfall totals in the higher rainfall zone, in the southern part of the study site. This wet bias in ERA5 is likely driven by challenges in the parametrisation of cumulus clouds and convection over steep topography (Steinkopf and Engelbrecht, 2022).

The seasonal rainfall maps show clearly varying rainfall amounts in different parts of South Africa. The rainfall is highest in the eastern region (the eastern escarpment) in the DJF season and decreases in the SON, JJA and MAM seasons, which is typical of a summer rainfall zone. On the other hand, the Western Cape and some parts of the southeastern Cape receive most of their rainfall during JJA, and some areas along the southern coast, including parts of the southeastern Cape, show rainfall peaks during JJA and MAM. That is, these areas lie in the winter rainfall zone of South Africa. However, the southeastern Cape more broadly exhibits a transitional or a-seasonal rainfall regime, with equinoctial peaks in some locations, as reported by Roffe et al. (2021). These patterns align with the broader rainfall zone classifications in South Africa previously defined by Schulze (1997) and Tyson and Preston-Whyte (2000), where different zones of South Africa have been classified as having summer, winter or all year round rainfall. The summer rainfall zone which covers most of the interior and the eastern parts of the country is governed by convective rainfall which is related to tropical-temperate troughs and synoptic-scale systems (Tyson and Preston-Whyte, 2000; Roffe et al., 2021). In contrast, the winter rainfall zone is limited to the southwestern Cape and is associated with mid-latitude cyclones and frontal systems. The year-round rainfall in the southeastern Cape is in the transitional zone where both synoptic systems and orographic factors determine the rainfall (Tyson and Preston-Whyte, 2000; Roffe et al., 2021).

The analysis of the seasonal rainfall shows that the north-south gradient over the eastern escarpment study site is mainly related to the DJF and SON seasons, and this is clear in both CRU and ERA5. Moreover, the examination of the seasonal rainfall patterns in ERA5 shows the same biases as those seen in the annual rainfall. That is, ERA5 overestimates rainfall in all the four seasons in most parts of South Africa. Particularly, over the eastern escarpment study site, a persistent wet bias is evident in the seasonal rainfall of ERA5. This overestimation has been ascribed to the satellite data assimilation methods that enhance the convective rainfall during the period of high precipitation (Gleixner et al., 2020). The results here support this, with the greatest biases seen during DJF, the rainy season, and SON, which is the second rainiest season. In contrast, the biases across the various seasons over the eastern escarpment study site are lowest in the JJA and MAM seasons, which further suggests that the bias is mainly through overestimation of convective rainfall. The regional differences in seasonal rainfall are important for understanding ERA5's performance in simulating seasonal rainfall, particularly the overestimation of convective rainfall in the

summer rainfall region and possible biases in the simulation of winter cyclone rainfall and orographic rainfall in the southwestern Cape.

The comparison of rainfall distributions and the extreme rainfall events is also useful to reveal the discrepancies between CRU and ERA5. The ERA5 rainfall distribution shows a stronger representation of higher levels of rainfall events compared to CRU, particularly at the upper end of the distribution . This therefore suggests that ERA5 is more effective in detecting short-term extreme events and therefore could be useful in early warning systems. However, previous studies (McPhaden, 2008; Bell et al., 2018) have reported that reanalysis datasets overestimate the occurrence of extreme rainfall events, particularly in the regions where rainfall is influenced by ENSO. These differences are further highlighted in the subregion statistical investigation. In particular, it can be seen that ERA5 overestimates rainfall in all the months and the bias is highest in the DJF and SON months, especially in the regions with complex topography such as the Drakensberg Mountains. On the other hand, ERA5 has a tendency to underestimate rainfall in the western interior and arid zones, where convective rainfall is less frequent. It is important to note that the greatest similarity between CRU and ERA5 is in the JJA season when convection is at its lowest.

6.3 ENSO-Rainfall Teleconnection: Implications and Variability

The climate of the southern African region is marked by significant year-to-year changes which are mainly due to the El Niño Southern Oscillation (ENSO), with the ENSO signal itself being seasonal (Nicholson and Kim, 1997). The well-established influence of ENSO events on rainfall in South Africa is negative rainfall anomalies during El Niño and positive rainfall anomalies during La Niña (Reason and Rouault, 2005; Alemaw and Chaoka, 2006; Dieppois et al., 2015). The results in this study confirm the ENSO teleconnection to rainfall over both South Africa and the eastern escarpment study site and reveal that ERA5 is able to capture the ENSO signal in rainfall. However, it should be noted that the magnitude of anomalies is overestimated by ERA5, especially during La Niña. The results further confirm that ENSO has the strongest influence during the DJF (summer) season when moisture advection and atmospheric circulation are most sensitive to ENSO anomalies (Reason and Rouault, 2005; Dieppois et al., 2015). While previous studies (such as Steinkopf and Engelbrecht (2022)) have shown that ERA5 is able to correctly capture the ENSO-rainfall teleconnection over Africa, the results here provided greater insights into the spatial

variability of the rainfall anomalies across South Africa and, in particular, the eastern escarpment study site.

The seasonal variability of the ENSO impacts on rainfall anomalies is highest during the austral summer (DJF). Previous work by Alemaw and Chaoka (2006) and Dieppois et al. (2015) established that ENSO affects rainfall in Southern Africa by controlling the strength and location of large-scale convergence of moisture. Specifically, El Niño events are seen to be associated with increased subsidence and a weakening of tropical-temperate troughs over the subcontinent, leading to suppressed convection and reduced rainfall over most of South Africa during the DJF season. Additionally, El Niño events are linked to the northward displacement of convergence zones, shifting moisture influx away from the region, which contributed to drier conditions in the eastern and central parts of South Africa during the DJF season (Mpheshea et al., 2025). These atmospheric processes are less active during the transition seasons of MAM and SON, which explains the reduced ENSO signal in the rainfall anomalies during these seasons. Crétat et al. (2019) found that the atmosphere is least sensitive to ENSO because of decoupling of the oceanic and atmospheric circulation systems during MAM, while Dieppois et al. (2015) established that the ENSO-related rainfall anomalies in southern Africa are most significant in the DJF season and that only residual or weak signals are present in the SON season.

In JJA (winter), ENSO has a limited impact on rainfall across most of South Africa, including the eastern escarpment study site as was shown by both CRU and ERA5. This is in agreement with Engelbrecht et al. (2020) and Reason and Rouault (2005) who claimed that ENSO has a moderate effect on the winter rainfall which is largely driven by mid-latitude frontal systems which control the winter rainfall zone in the southwestern parts of South Africa. However, Reason and Rouault (2005) and Dieppois et al (2015) offer a more nuanced perspective, showing that strong El Niño events can lead to increased rainfall in the Western Cape region due to associated subsidence anomalies and a southward displacement of the westerly storm tracks. This shift can hinder the progression of frontal systems into the winter rainfall zone (Rouault et al., 2024). This suggests that, even though ENSO's effect is less significant in the central and eastern parts of South Africa during the winter season, as determined by this study, it can affect rainfall in the southwestern Cape, depending on the intensity of ENSO and its simultaneous interactions with other climate drivers such as the Southern Annular Mode (SAM) and the Indian Ocean Dipole (IOD)

(Reason and Rouault, 2005; Behera et al., 2005). Therefore, ENSO's influence on winter rainfall is not uniform across the country but instead exhibits spatial variability.

This research indicates that the influence of ENSO on rainfall varies substantially across South Africa, with the eastern escarpment showing the strongest anomalies. Specifically, in both the ranked ENSO-event analysis and DFJ seasonal composites, rainfall anomalies in this region were larger than in the lowland or western areas. This spatial pattern is consistent with the fact that the Drakensberg Mountains enhance rainfall variability through orographic uplift, especially during ENSO events (Taylor et al., 2016). Orographic processes intensify precipitation on the windward slopes when ENSO-related changes in moisture transport strengthen easterly inflow, while lee-side regions experience reduced rainfall (Taylor et al., 2016; Engelbrecht et al., 2020). The importance of the Drakensberg region for water resources is well-documented because it supplies runoff to the Tugela and Orange rivers, and ENSO-related rainfall anomalies in this catchment can affect seasonal river flows and groundwater recharge which determines water supply (Alemaw and Chaoka, 2006). However, the extent to which climate models accurately represent these interactions continues to be difficult because coarse-resolution models have a limited ability to detect the detailed terrain and local precipitation patterns (Blamey and Reason, 2023). Improving our understanding of ENSO-rainfall dynamics, particularly over regions of complex topography, is therefore essential for enhancing seasonal rainfall predictions and water security management in southern Africa, with the consideration of future climate change scenarios.

Finally, while ENSO is widely acknowledged as the dominant driver of rainfall variability over the southern African region (including the eastern escarpment study site), particularly during DJF, year-to-year deviations from the typical ENSO signal are evident. For example, the CRU dataset shows above-average DJF rainfall over the study site during the El Niño events of 1997/8, 2004/5, and 2009/10, while ERA5 highlights 2004/5 as having a strong positive anomaly. Furthermore, negative DJF rainfall anomalies are recorded in CRU, over the study site, during numerous La Niña events, and the same is true for ERA5. Some El Niño years do not lead to drought, and some La Niña years fail to produce widespread wet conditions. This variability can be explained by additional factors such as the Indian Ocean Dipole (Behera et al., 2005), local SST anomalies (Trenberth, 1997), and sub-seasonal systems like the Madden–Julian Oscillation (McPhaden, 2008), which can either amplify or suppress ENSO-driven convection. Recent work by Blamey and Reason (2023) further

emphasises that the diversity of ENSO events, particularly differences between Eastern-Pacific and Central-Pacific El Niño types along with regional atmospheric features such as the Botswana High and moisture flux patterns, significantly influence rainfall outcomes in southern Africa. Their findings show that even during strong ENSO events, regional climate anomalies may not align with expected patterns due to complex interactions between large-scale drivers and local circulation. These insights highlight the importance of using multiple datasets and considering the broader climate context when evaluating ENSO's impact on regional rainfall variability.

6.4 Regional Disparities in ENSO Impact

ENSO is widely regarded as one of the dominant large-scale climate drivers influencing rainfall variability in South Africa, particularly during the austral summer (DJF) (Landman et al., 2001,). El Niño is typically associated with below-normal rainfall and drought while La Niña is typically associated with above-normal rainfall. Nonetheless, the size of these anomalies and the places where they occur differ considerably from one event to the next and are shaped by local factors (Engelbrecht et al., 2020; Reason and Rouault, 2005; Dieppois et al., 2015). The results of this research show that the eastern escarpment study site exhibits relatively stronger ENSO-related rainfall anomalies compared to other parts of the region . Taylor et al. (2016) and Engelbrecht et al. (2015) also found that regional topography enhances the hydrological impact of ENSO, especially in regions such as the Drakensberg. Precipitation in the area is sensitive to variations in atmospheric moisture transport and therefore the escarpment is an area of particular interest in ENSO-driven hydroclimatic variation. Reason and Rouault (2005) also noted that the interactions with synoptic systems at the local scale either enhance or weaken the manifestation of ENSO anomalies, thereby pointing to the importance of spatial context.

As previously stated, not all ENSO events were associated with the expected rainfall conditions. Both CRU and ERA5 datasets indicate that some individual El Niño and La Niña events exhibited opposite rainfall responses, with above-normal rainfall in certain El Niño years and below-normal rainfall during some La Niña events. These inconsistencies suggest that ENSO's influence on rainfall can be modulated or overridden by other climate drivers. Behera et al. (2005) and Engelbrecht et al. (2020) also observed that while ENSO alters the intensity and direction of tropical moisture plumes, such impacts are not always

straightforward. IOD anomalies or variability in the SAM can either amplify or weaken the changes in the circulation due to ENSO, which in turn can affect rainfall anomalies These complexities are evident in our comparative analysis of CRU and ERA5 datasets, which generally align on ENSO trends but differ in the magnitude of anomalies, especially during La Niña phases. This reinforces the need to interpret ENSO's impacts within the broader multi-scale climate system rather than in isolation.

Rainfall patterns in South Africa are also affected by other climate drivers such as Madden–Julian Oscillation (MJO), Pacific Decadal Oscillation (PDO), and Indian Ocean SST anomalies. These interactions not only influence the development and intensity of ENSO events themselves but also shape the regional impacts on rainfall (McPhaden et al., 2006). The MJO, in particular, modulates convective activity on intra-seasonal timescales which may affect the timing and distribution of rainfall during ENSO years. These dynamic interactions can also explain why some ENSO years do not follow the expected rainfall signal.

The research conducted by Blamey and Reason (2023) demonstrates the complexity of ENSO impacts on the eastern coast of subtropical southern Africa. According to their research, ENSO controls rainfall patterns significantly in this region, but its influence remains uneven across different areas and its intensity differs between regions. For example, the relationship between Niño 3.4 and summer rainfall is stronger in some locations than others, and certain ENSO events produced unexpected rainfall anomalies, indicating the role of additional modulating factors. These results support the notion that ENSO's impact is not uniform across South Africa and that climate dynamics, including interactions with the Indian Ocean Dipole (IOD) and Southern Annular Mode (SAM), can alter expected rainfall outcomes. The study demonstrates the need for multi-dataset evaluation and event classification (e.g. EP vs CP El Niño) to improve forecasting accuracy of hydroclimatic patterns in South Africa.

6.5 Implications for Climate Science and Water Resource Management

This study provides evidence that ENSO is one of the primary drivers of interannual rainfall variability across South Africa, with the strongest anomalies observed over the eastern escarpment study site. It is also clear that ENSO is a vital predictor of seasonal rainfall

anomalies. However, ENSO's influence is not uniform across South Africa, the western interior and southwestern Cape regions show weaker ENSO correlations due to their dominant winter rainfall regime, which is influenced more by mid-latitude westerlies than tropical teleconnections (Reason and Rouault, 2005). The strength of the ENSO signal over the eastern escarpment study site has important implications for water resource management in South Africa.

The eastern escarpment serves as an important water region for South Africa, which feeds major river systems such as the Tugela and Orange (Taylor et al., 2016). Reliable seasonal forecasts based on ENSO signals can enhance water management strategies by informing reservoir operations, optimising water allocations, and improving early warning systems for both droughts and floods. This is especially critical in the context of increasing climate variability and growing water demand. These findings align with Taylor et al. (2016) and Engelbrecht et al. (2015), who emphasise the need for improved forecasting tools in climate-sensitive source regions to mitigate hydrological risks. Furthermore, the results highlight the importance of integrating climate knowledge into long-term infrastructure planning, especially in water-stressed provinces where ENSO-driven variability can significantly influence streamflow, soil moisture, and groundwater recharge (Engelbrecht et al., 2020). Strengthening predictive capabilities in these regions can support more resilient water management and adaptation strategies in a changing climate.

Validating ERA5 against observational datasets like CRU is crucial for future climate model development, as many models are benchmarked against ERA5 reanalysis. Since climate models rely on reanalysis data to calibrate and validate their simulations, assessing how well ERA5 represents ENSO-driven rainfall variability ensures that these models are built on a robust foundation. If ERA5 accurately captures ENSO teleconnections, it strengthens confidence in its use as a reference dataset for global and regional climate simulations. Conversely, any biases or inconsistencies identified in ERA5 provide critical insights for improving model parameterizations and correcting systematic errors. Given that ENSO plays a fundamental role in modulating southern African rainfall, ensuring that ERA5 reliably reproduces these relationships enhances the credibility of climate projections, particularly under future warming scenarios. This is because ERA5 is often used to validate and calibrate climate models. If it captures ENSO impacts accurately, we can have more

confidence in future projections and their use in seasonal forecasting, water planning, and climate adaptation.

Chapter 7: Conclusion

7.1 Assessment of the achievement of the aim and objectives

This study aimed to investigate the spatial and temporal characteristics of rainfall in South Africa's mega-dam region and assess the influence of ENSO on precipitation anomalies. A key focus was evaluating how well the ERA5 reanalysis dataset captures ENSO-rainfall teleconnections compared to observational data (CRU). By analysing how rainfall patterns change across different ENSO phases and seasons, this study provides critical insights into climate variability, dataset reliability, and the implications for seasonal forecasting and water resource management in this hydrologically significant region.

The first objective of this study was to quantify the ENSO-rainfall relationship over the eastern escarpment region using the observational dataset. The results confirm that during El Niño events, the eastern escarpment study site is associated with dry conditions (below-normal rainfall) and during La Niña events wet conditions (above-normal rainfall) occur. This relationship between rainfall and ENSO phases has been well-studied over southern Africa as a whole, but this study provides new insights at the regional scale. The influence of ENSO on rainfall over South Africa is strongest during austral summer season (DJF), and much weaker in the other seasons, and it is interesting to note that this holds true for the eastern escarpment study site too. Moreover, the eastern escarpment area has some spatial variability in the rainfall response during spring (SON) and not all the areas have the same pattern of above- or below-normal rainfall, although the anomalies are generally small. In terms of observations, another key finding is the shift to positive (negative) rainfall anomalies during El Niño (La Niña) events in winter (JJA). This was also consistent both country-wide and over the eastern escarpment region. However, given the limited winter rainfall over the eastern escarpment, this suggests that ENSO is not the primary driver of precipitation during this season. The second objective was to determine how well the ERA5 dataset captures the ENSO-rainfall teleconnection over the eastern escarpment region. This comparison with the CRU dataset indicates that ERA5 captures the well-known ENSO-linked rainfall anomalies reasonably well, with the expected dry (wet) conditions during El Niño (La Niña) events in the DJF period. The dataset performs effectively in capturing the spatial patterns and the seasonal rainfall responses, particularly during the austral summer. Nonetheless, ERA5 is prone to overemphasise the magnitude of anomalies,

especially during La Niña years, and has a general wet bias over the escarpment. Having said this, the high correlation between ERA5 and CRU during DJF indicates that ERA5 is a suitable model to represent the ENSO impacts in this environmentally complex region, although absolute values should be used with some caution.

The third objective was to compare historical El Niño and La Niña events to see how they differ in their impacts on rainfall in the mega-dam region. The analysis further reveals that while El Niño leads to below-normal rainfall, and La Niña leads to above-normal rainfall, this is not always the case across all the years. Some El Niño years had near-normal or even above-normal rainfall in the study area and not all La Niña events resulted in consistent wet conditions. These differences in event variations show the involvement of other climate factors and atmospheric conditions in the modulation of ENSO effects.

The findings of this study have important implications for water resource management and seasonal forecasting. The persistent ENSO–rainfall relationship in the eastern escarpment suggests the potential value of ENSO-based seasonal forecasting in this region, which serves as a key source area for major river systems. This understanding of these teleconnections may be useful for enhancing early warning systems, improving the management of reservoirs, and in supporting climate-resilient water planning. However, the variability in rainfall responses across different ENSO events underscore the need for careful interpretation of seasonal forecasts and the integration of different data sources. While ERA5 provides valuable spatial and temporal resolution that can assist in identifying rainfall anomalies, its tendency to overestimate rainfall totals suggests that bias correction is necessary for its effective application in climate models. Given that ENSO has the greatest influence on rainfall over the study site during DJF, with a moderate signal in SON, these seasons should be prioritised in seasonal forecasting and drought risk management strategies. Overall, this study demonstrates the usefulness of both reanalysis and observational datasets to obtain reliable insights into regional hydroclimatic behaviour.

7.2 Study Limitations and Future Research Directions

While this study provides valuable insights into ENSO's influence on South African rainfall, several limitations should be acknowledged. As a first step, it is worthwhile to expand the observational baseline by incorporating more rainfall datasets. Although CRU is a good gridded observational product, it is not always accurate in regions with limited station

coverage. Employing multiple observational sources would increase the certainty of the results and the robustness of the ENSO–rainfall analyses. In addition, while this study focused on ENSO as the main climate driver, other large-scale systems such as the Indian Ocean Dipole, the Southern Annular Mode, and the Madden–Julian Oscillation can also affect rainfall variability in the region. How these modes combine with ENSO would be useful in refining the seasonal forecasting models and increasing understanding of compound climate effects. There is a need to carry out a follow-up study to determine how the ENSO–rainfall teleconnection may shift with future climate scenarios. Such a study would be useful for informing long-term water resource planning and climate adaptation strategies in South Africa, which would be especially valuable if repeated using CMIP6 global climate models to help understand whether the strength, frequency, or spatial expression of ENSO-linked rainfall anomalies is likely to change with a changing climate.

7.3 Final Thoughts

Based on the outcome of this research, it is important that future work builds on this study by employing global climate models and more observational data. A direction that could be worth pursuing in the future is to perform this analysis again using the output of CMIP6 (Sixth Coupled Climate Model Intercomparison Project) global climate models to see how the ENSO rainfall relationship over the eastern escarpment is projected to change with different climate change scenarios. It could be helpful to determine if the teleconnection is probably going to get stronger, weaker or even move to some other area. There is a need to improve the calibration and bias correction of reanalysis products like ERA5, especially in the complex terrain where overestimation of rainfall can lead to incorrect assumptions in water management. Lastly, it is important that future work should combine climate science with hydrology, agriculture and disaster risk management to develop more integrated and multidisciplinary approaches to provide recommendations for adaptation measures. These efforts will be crucial to improving climate resilience in the region in a future of increased variability and uncertainty.

References

AghaKouchak, A., Farahmand, A., Melton, F. S., Teixeira, J., Anderson, M. C., Wardlow, B. D., & Hain, C. R. (2015). Remote sensing of drought: Progress, challenges and opportunities. Reviews of Geophysics, 53(2), 452–480.

Alemaw, B. F., & Chaoka, T. R. (2006). The 1950–1998 warm ENSO events and regional implications to river flow variability in Southern Africa. Water SA, 32(4), 459–464.

Alemaw, B. F. (2022). The recent droughts of 2019/20 in Southern Africa and its teleconnection with ENSO events. *Atmospheric and Climate Sciences, 12*(2), 246–263.

Anyamba, A., Tucker, C. J., & Mahoney, R. (2002). From El Niño to La Niña: Vegetation response patterns over East and Southern Africa during the 1997–2000 period. Journal of Climate, 15(21), 3096–3103. https://doi.org/10.1175/1520-0442(2002)015

Barnston, A. G., Chelliah, M., & Goldenberg, S. B. (1997). Documentation of a highly ENSO-related SST region in the equatorial Pacific. *Atmosphere-Ocean, 35*(3), 367–383. https://doi.org/10.1080/07055900.1997.9649597

Barber, R.T., & Chavez, F.P. (1983). Biological consequences of El Niño. Science, 222(4629), 1203-1210. https://doi.org/10.1126/science.222.4629.1203

Barnston, A.G., Glantz, M.H., & He, Y. (1999). Predictive skill of statistical and dynamical climate models in SST forecasts during the 1997–98 El Niño episode and the 1998 La Niña onset. Bulletin of the American Meteorological Society, 80(2), 217-243.

Barnston, A. G., Glantz, M. H., & He, Y. (1999). Predictive skill of statistical and dynamical climate models in SST forecasts during the 1997–98 El Niño episode and the 1998 La Niña onset. *Bulletin of the American Meteorological Society, 80*(2), 217–244.

Bayer, A. M., Danysh, H. E., Garvich, M., Gonzálvez, G., Checkley, W., Alvarez, M., & Gilman, R. H. (2014). An unforgettable event: A qualitative study of the 1997–98 El Niño in northern Peru. *Disasters, 38*(2), 351–374. https://doi.org/10.1111/disa.12046

Beharie (Rampath), S. (2019). *Climate-related societal consequences and responses during the 19th century, South Africa and Lesotho, 1830–1900* (Master's thesis). University of the Witwatersrand, Johannesburg, South Africa.

Behera, S. K., Luo, J.-J., Masson, S., Delecluse, P., Gualdi, S., Navarra, A., & Yamagata, T. (2005). Paramount impact of the Indian Ocean Dipole on the East African short rains: A CGCM study. Journal of Climate, 18(21), 4514–4530. https://doi.org/10.1175/JCLI3541.1

Behera, S. K., Salvekar, P. S., & Yamagata, T. (2000). Simulation of interannual SST variability in the tropical Indian Ocean. *Journal of Climate, 13*(19), 3487–3499.

Bell, J. D., Allain, V., Sen Gupta, A. S., Johnson, J. E., Hampton, J., Hobday, A. J., Lehodey, P., Lenton, A., Moore, B. R., Pratchett, M. S., Senina, I., Smith, N., & Williams, P. (2018). Climate change impacts, vulnerabilities and adaptations: Western and Central Pacific Ocean marine fisheries. In M. Barange, T. Bahri, M. C. M. Beveridge, K. L. Cochrane, S. Funge-Smith, & F. Poulain (Eds.), *Impacts of climate change on fisheries and aquaculture: Synthesis of current knowledge, adaptation and mitigation options* (FAO Fisheries and Aquaculture Technical Paper No. 627, pp. 305–324). FAO.

Benhin, J. K. A. (2006). *Climate change and South African agriculture: Impacts and adaptation options* (CEEPA Discussion Paper No. 21). Centre for Environmental Economics and Policy in Africa, University of Pretoria. [PDF].

Binns, J.A., Illgner, P.M., & Nel, E.L. (2001). Water shortage, deforestation, and development: South Africa's working for water programme. Land Degradation & Development, 12(4), 341-355. https://doi.org/10.1002/ldr.455

Blamey, R. C., & Reason, C. J. C. (2023). Diversity and ranking of ENSO impacts along the eastern seaboard of subtropical southern Africa. *Atmosphere, 14*(6), 1042.

Bonsal, B.R., Shabbar, A., & Higuchi, K. (2001). Impacts of low-frequency variability modes on Canadian winter temperature. International Journal of Climatology, 21(1), 95-108. https://doi.org/10.1002/joc.590

Brugnara, Y., Brönnimann, S., Grab, S., Steinkopf, J., Burgdorf, A.-M., Wilkinson, C., & Allan, R. (2023). South African extreme weather during the 1877–1878 El Niño. *Weather, 78*(10), 286–293. https://doi.org/10.1002/wea.4468

Cai, W., … Zhong, W. (2021). Changing El Niño–Southern Oscillation in a warming climate. *Nature Reviews Earth & Environment, 2*(9), 628–644.

Castrejón, M., Pittman, J., Ramírez-González, J., & Defeo, O. (2024). An overview of social-ecological impacts of the El Niño–Southern Oscillation and climate change on Galapagos small-scale fisheries. *Ocean & Coastal Management, 259*, 107436. https://doi.org/10.1016/j.ocecoaman.2024.107436

Chen, D., & Cane, M. A. (2008). El Niño prediction and predictability. *Journal of Computational Physics, 227*(7), 3625–3640. https://doi.org/10.1016/j.jcp.2007.05.014

Chen, H., Jin, Y., Liu, Z., Sun, D., Chen, X., McPhaden, M. J., Capotondi, A., & Lin, X. (2024). Central-Pacific El Niño–Southern Oscillation less predictable under greenhouse warming. *Nature Communications, 15*, 4370. https://doi.org/10.1038/s41467-024-48804-1

Chen, Y., Zhao, C., & Zhi, H. (2024). Analysis of ENSO event intensity changes and time–frequency characteristic since 1875. Atmosphere, 15(12), 1428.

Climatic Research Unit (CRU). (2023). *CRU TS4.06: Climatic Research Unit (CRU) Time-Series (TS) version 4.06 dataset*. University of East Anglia. https://crudata.uea.ac.uk/cru/data/hrg/

Collins, M., An, S.-I., Cai, W., Ganachaud, A., Guilyardi, E., Jin, F.-F., Jochum, M., Lengaigne, M., Power, S., Timmermann, A., Vecchi, G., & Wittenberg, A. (2010). The impact of global warming on the tropical Pacific Ocean and El Niño. Nature Geoscience, 3(6), 391–397.

Crétat, J., Pohl, B., Dieppois, B., Berthou, S., & Pergaud, J. (2019). The Angola Low: relationship with southern African rainfall and ENSO. Climate Dynamics, 52, 1783–1803.

Crétat, J., Richard, Y., Pohl, B., Rouault, M., Reason, C., & Fauchereau, N. (2010). Recurrent daily rainfall patterns over South Africa and associated dynamics during the core of the austral summer. International Journal of Climatology, 32(2), 261–273.

Dee, D. P., Uppala, S. M., Simmons, A. J., Berrisford, P., Poli, P., Kobayashi, S., Andrae, U., Balmaseda, M. A., Balsamo, G., Bauer, P., Bechtold, P., Beljaars, A. C. M., van de Berg, L., Bidlot, J., Bormann, N., Delsol, C., Dragani, R., Fuentes, M., Geer, A. J., Haimberger, L., ... Thépaut, J.-N. (2011). The ERA-Interim reanalysis: configuration and performance of the data assimilation system. *Quarterly Journal of the Royal Meteorological Society*, 137(656), 553–597.

Dieppois, B., Pohl, B., & Rouault, M. (2015). The impact of ENSO on Southern African rainfall in CMIP5 ocean-atmosphere coupled climate models. Climate Dynamics, 45(9-10), 2425-2442.

DiNezio, P. N., Deser, C., Karspeck, A., Yeager, S., Okumura, Y., Danabasoglu, G., Rosenbloom, N., Caron, J., & Meehl, G. A. (2017). A two-year forecast for a 60–80 % chance of La Niña in 2017–18. Geophysical Research Letters, 44(22), 11,624–11,635.

Doblas-Reyes, F. J., Sörensson, A. A., Almazroui, M., Dosio, A., Gutowski, W. J., Haarsma, R., Hamdi, R., Hewitson, B., Kwon, W.-T., Lamptey, B. L., Maraun, D., Stephenson, T. S., Takayabu, I., Terray, L., Turner, A., & Zuo, Z. (2021). Linking global to regional climate change. In V. Masson-Delmotte, P. Zhai, A. Pirani, S. L. Connors, C. Péan, S. Berger, N. Caud, Y. Chen, L. Goldfarb, M. I. Gomis, M. Huang, K. Leitzell, E. Lonnoy, J. B. R. Matthews, T. K. Maycock, T. Waterfield, O. Yelekçi, R. Yu, & B. Zhou (Eds.), Climate Change 2021: The Physical Science Basis. Contribution of Working Group I to the Sixth Assessment Report of the Intergovernmental Panel on Climate Change (pp. 1363–1512). Cambridge University Press.

Earle, A., Malzbender, D., Turton, A., & Manzungu, E. (2005). A Preliminary Basin Profile of the Orange/Senqu River. African Water Issues Research Unit (AWIRU), Centre for International Political Studies, University of Pretoria, Pretoria, South Africa, 44 pp. ISBN 1-86854-618-7.

Enfield, D. B. (1992). Historical and prehistorical overview of El Niño/Southern Oscillation. In H. F. Diaz & V. Markgraf (Eds.), El Niño: Historical and Paleoclimatic Aspects of the Southern Oscillation (pp. 95–117). Cambridge University Press.

Engelbrecht, C.J., Landman, W.A., Engelbrecht, F.A., & Malherbe, J. (2015). A synoptic decomposition of rainfall over the Cape south coast of South Africa. Climate Dynamics, 44, 2589-2607.

Engelbrecht, F., Dedekind, Z., Muthige, M., Malherbe, J., Beraki, A., Engelbrecht, C., Ngwana, I., Lumsden, T., Landman, W., Maisha, R., Mpheshea, L., van der Merwe, J., & Eatwell, K. (2020). Predictability of hydroclimatic variability over eastern South Africa under climate change. Water Research Commission Report No. 2457/1/20.

Gill, A. E. (1980). Some simple solutions for heat-induced tropical circulation. Quarterly Journal of the Royal Meteorological Society, 106(449), 447-462.

Gleixner, S.; Demissie, T.; & Diro, G. T. (2020). Did ERA5 improve temperature and precipitation reanalysis over East Africa? Atmosphere, 11(9), 996.

Glantz, M.H. (2002). La Niña and its impacts: Facts and speculation. United Nations University Press.

Hanley, D. E., Bourassa, M. A., O'Brien, J. J., Smith, S. R., & Spade, E. R. (2003). A quantitative evaluation of ENSO indices. Journal of Climate, 16(8), 1249-1258.

Harris, I., Osborn, T. J., Jones, P., & Lister, D. (2020). Version 4 of the CRU TS monthly high-resolution gridded multivariate climate dataset. *Scientific Data*, 7, Article 109.

Hart, N.C.G., Washington, R., & Reason, C.J.C. (2018). On the likelihood of tropical–extratropical cloud bands in the south Indian convergence zone during ENSO events. Journal of Climate, 31(7), 2797–2817.

Hersbach, H., Bell, B., Berrisford, P., Hirahara, S., Horányi, A., Muñoz‐Sabater, J., Nicolas, J., Peubey, C., Radu, R., Schepers, D., Simmons, A., Soci, C., Abdalla, S., Abellan, X., Balsamo, G., Bechtold, P., Biavati, G., Bidlot, J., Bonavita, M., … Thépaut, J.‐N. (2020). The ERA5 global reanalysis. Quarterly Journal of the Royal Meteorological Society, 146(730), 1999–2049.

Hlalele, B. M., & Makhubele, J. (2024). Precipitation variability determinants in the highlands of Lesotho. Water Conservation & Management, 8(4), 402-407.

Hund, S. V., Grossmann, I., Steyn, D. G., Allen, D. M., & Johnson, M. S. (2021). Changing water resources under El Niño, climate change, and growing water demands in seasonally dry tropical watersheds. Water Resources Research, 57(9), e2020WR028535.

Impson, N.D., Bills, I.R., & Wolhuter, L. (2007). Technical Report on the State of Yellowfishes in South Africa. Water Research Commission, Report No. KV 212/08. Pretoria: Water Research Commission.

Jones, C., & Carvalho, L. M. V. (2002). Active and break phases of the South American monsoon system. Journal of Climate, 15(8), 905–914.

Kao, H.Y., & Yu, J.Y. (2009). Contrasting Eastern-Pacific and Central-Pacific types of ENSO. Journal of Climate, 22(3), 615-632.

Kessler, W. S. (2006). The circulation of the eastern tropical Pacific: A review. Progress in Oceanography, 69(2-4), 181-217.

Landman, W. A., & Beraki, A. F. (2015). On the comparison between seasonal predictive skill of global circulation models: Coupled versus uncoupled. Journal of Geophysical Research: Atmospheres, 120(13), 5263–5281.

Landman, W.A., Mason, S.J., Tyson, P.D., & Tennant, W.J. (2001). Retro‐active skill of multi‐tiered forecasts of summer rainfall over southern Africa. International Journal of Climatology, 21(1), 1–19.

Latif, M., Anderson, D., Barnett, T., Cane, M., Kleeman, R., Leetmaa, A., O'Brien, J., Rosati, A., & Schneider, E. (1998). A review of the predictability and prediction of ENSO. Journal of Geophysical Research: Oceans, 103(C7), 14375-14393.

Lee, T., & McPhaden, M. J. (2010). Increasing intensity of El Niño in the central‐equatorial Pacific. Geophysical Research Letters, 37(14), L14603.

Lee, J.-Y., J. Marotzke, G. Bala, L. Cao, S. Corti, J.P. Dunne, F. Engelbrecht, E. Fischer, J.C. Fyfe, C. Jones, A. Maycock, J. Mutemi, O. Ndiaye, S. Panickal, and T. Zhou (2021). Future Global Climate: Scenario-Based Projections and Near-Term Information. In: *Climate Change 2021: The Physical Science Basis. Contribution of Working Group I to the Sixth Assessment Report of the Intergovernmental Panel on Climate Change* [Masson-Delmotte, V., P. Zhai, A. Pirani, S.L. Connors, C. Péan, S. Berger, N. Caud, Y. Chen, L. Goldfarb, M.I. Gomis, M. Huang, K. Leitzell, E. Lonnoy, J.B.R. Matthews, T.K. Maycock, T. Waterfield, O. Yelekçi, R. Yu, and B. Zhou (eds.)].

L'Heureux, M. L., Tippett, M. K., Wheeler, M. C., Nguyen, H., Narsey, S., Johnson, N., Hu, Z.-Z., Watkins, A. B., Lucas, C., Ganter, C., Becker, E., Wang, W., & Di Liberto, T. (2024). A relative sea surface temperature index for classifying ENSO events in a changing climate. Journal of Climate, 37(4), 1197-1211. https://doi.org/10.1175/JCLI-D-23-0406.1

Li, M., Xu, Y., Sun, M., Li, J., Zhou, X., Chen, Z., & Zhang, K. (2023). Impacts of strong ENSO events on fish communities in an overexploited ecosystem in the South China Sea. Biology (Basel), 12(7), 946.

Lin, H., Muncaster, R., Derome, J., Merryfield, W. J., & Diro, G. (2024). Skillful long-lead seasonal predictions in the summertime Northern Hemisphere midlatitudes. Journal of Climate, 37(18), 4915-4929. https://doi.org/10.1175/JCLI-D-24-0097.1

Lindzen, R. S., & Nigam, S. (1987). On the role of sea surface temperature gradients in forcing low-level winds and convergence in the tropics. Journal of the Atmospheric Sciences, 44(17), 2418-2436.

Liu, Y., Cai, W., Lin, X., Li, Z., & Zhang, Y. (2023). Nonlinear El Niño impacts on the global economy under climate change. Nature Communications, 14, Article 5791.

Lyon, B., & Mason, S. J. (2009). The 1997/98 summer rainfall season in Southern Africa. Part II: Model simulations and coupled model forecasts. Journal of Climate, 22(13), 3802–3818. https://doi.org/10.1175/2009JCLI2600.1

Matewos, T. (2019). Climate change-induced impacts on smallholder farmers in selected districts of Sidama, Southern Ethiopia. Climate, 7(5), 70. https://doi.org/10.3390/cli7050070

Mathinya, N. V., Clark, V. R., van Tol, J. J., & Franke, A. C. (2022). Resilience and sustainability of the Maloti-Drakensberg mountain system: A case study on the Upper uThukela catchment. In I. Misiune, D. Depellegrin, & L. E. Vigl (Eds.), Human-Nature Interactions: Exploring Nature's Values Across Landscapes (pp. 155–167). Springer Nature, Cham. https://doi.org/10.1007/978-3-031-01980-7_13

Mbiriri, M., Mukwada, G., & Manatsa, D. (2018). Influence of altitude on the spatiotemporal variations of meteorological droughts in mountain regions of the Free State Province, South Africa (1960–2013). Advances in Meteorology, 2018, Article 5206151. https://doi.org/10.1155/2018/5206151

McPhaden, M. J., Zebiak, S. E., & Glantz, M. H. (2006). ENSO as an integrating concept in earth science. Science, 314(5806), 1740–1745. https://doi.org/10.1126/science.1132588

McPhaden, M. J. (2008). Evolution of the 2006–2007 El Niño: The role of intraseasonal to interannual time-scale dynamics. Advances in Geosciences, 14, 219–230.

Lee, T., & McPhaden, M. J. (2010). Increasing intensity of El Niño in the central-equatorial Pacific. Geophysical Research Letters, 37(14), L14603.

Meyers, G., McIntosh, P., Pigot, L., & Pook, M. (2007). The years of El Niño, La Niña, and interactions with the tropical Indian Ocean. Journal of Climate, 20(13), 2872–2880.

Mpheshea, L. E., Blamey, R. C., & Reason, C. J. C. (2025). The influence of ENSO-type on rainfall characteristics over southern Africa during the austral summer. Climate Dynamics, 63, Article 161.

Nash, D. J., & Grab, S. W. (2010). “A sky of brass and burning winds”: Documentary evidence of rainfall variability in the Kingdom of Lesotho, Southern Africa, 1824–1900. Climatic Change, 101(3–4), 617–653. https://doi.org/10.1007/s10584-009-9707-y

Nhemachena, C., Nhamo, L., Matchaya, G., Nhemachena, C. R., Muchara, B., Karuaihe, S. T., & Mpandeli, S. (2020). Climate change impacts on water and agriculture sectors in Southern Africa: Threats and opportunities for sustainable development. Water, 12(10), Article 2673. https://doi.org/10.3390/w12102673

Nicholson, S. E. (2017). Climate and climatic variability of rainfall over eastern Africa. Reviews of Geophysics, 55(3), 590–635. https://doi.org/10.1002/2016RG000544

Nicholson, S. E., & Kim, J. (1997). The relationship of the El Niño–Southern Oscillation to African rainfall. International Journal of Climatology, 17(2), 117–135.

Niinuma, T., & Yasuda, I. (2025). Eastward propagation of mid‐latitude near‐surface thermohaline anomaly and link to marine heat waves in the eastern North Pacific. Journal of Oceanography, 81(1), 41–61.

NOAA Climate Prediction Center (CPC). (n.d.). Oceanic Niño Index (ONI). Retrieved from https://origin.cpc.ncep.noaa.gov/products/analysis_monitoring/ensostuff/ONI_v5.php

Palmer, P. I., Wainwright, C. M., Dong, B., Maidment, R. I., Wheeler, K. G., Gedney, N., … Turner, A. G. (2023). Drivers and impacts of Eastern African rainfall variability. Nature Reviews Earth & Environment, 4(4), 254–270. https://doi.org/10.1175/JCLI-D-23-0637.1

Pan, L., Wang, X., Chen, J., & Zhan, H. (2024). Distinct features of tropical cyclone landfall over East Asia during various types of El Niño. Journal of Climate, 37(19), 7727–7749.

Philander, S. G. (2001). El Niño Southern Oscillation (ENSO) models. In Encyclopedia of Ocean Sciences (1st ed., pp. 827–832). Academic Press.

Qu, C., Hao, X., & Qu, J. J. (2019). Monitoring Extreme Agricultural Drought over the Horn of Africa (HOA) using remote sensing measurements. Remote Sensing, 11(8), 902.

Ranasinghe, R., Ruane, A. C., Vautard, R., Arnell, N., Coppola, E., Cruz, F. A., … Wang, W. (2021). Climate change information for regional impact and for risk assessment. In V. Masson-Delmotte et al. (Eds.), Climate Change 2021: The Physical Science Basis (IPCC AR6 WGI), pp. 1767–1926. Cambridge University Press.

Reason, C. J. C., & Rouault, M. (2005). Links between the Antarctic Oscillation and winter rainfall over western South Africa. Geophysical Research Letters, 32(7), L07705.

Roffe, S. J., Fitchett, J. M., & Curtis, C. J. (2021). Investigating changes in rainfall seasonality across South Africa: 1987–2016. International Journal of Climatology, 41(S1), E2031–E2050.

Rouault, M., Dieppois, B., Tim, N., Hünicke, B., & Zorita, E. (2024). Southern Africa climate over the recent decades: Description, variability and trends. In B. Dieppois, C. J. C. Reason, & C. Lennard (Eds.), Sustainability of Southern African Ecosystems under Global Change (pp. 149–168). Springer. https://doi.org/10.1007/978-3-031-10948-5_6

Saurral, R. I., García-Serrano, J., Doblas-Reyes, F. J., & Díaz, L. B. (2020). Decadal predictability and prediction skill of sea surface temperatures in the South Pacific region. Climate Dynamics, 54(11–12), 3945–3958.

Sazib, N., Bolten, J., & Mladenova, I. (2020). Exploring spatiotemporal relations between soil moisture, precipitation, and streamflow for a large set of watersheds using Google Earth Engine. Water, 12(5), 1371. https://doi.org/10.3390/w12051371

Steinkopf, J., & Engelbrecht, F. A. (2022). Verification of ERA5 and ERA-Interim precipitation over Africa at intra-annual and interannual timescales. Atmospheric Research, 280, 106427. https://doi.org/10.1016/j.atmosres.2022.106427

Schulze, R. E. (1997). South African Atlas of Agrohydrology and Climatology. Water Research Commission, Report No. TT82/96. Pretoria, South Africa.

Taylor, S. J., Ferguson, J. W. H., Engelbrecht, F. A., Clark, V. R., Van Rensburg, S., & Barker, N. (2016). The Drakensberg Escarpment as the great supplier of water to South Africa. In G. Greenwood & J. Shroder (Eds.), Mountain Ice and Water: Investigations of the Hydrologic Cycle in Alpine Environments (Developments in Earth Surface Processes, Vol. 21, pp. 1–46). Elsevier. https://doi.org/10.1016/B978-0-444-63787-1.00001-9

Trenberth, K. E. (1997). The definition of El Niño. Bulletin of the American Meteorological Society, 78(12), 2771–2777.

Trenberth, K. E., & Stepaniak, D. P. (2001). Indices of El Niño evolution. Journal of Climate, 14(8), 1697–1701.

Trenberth, K. E., & Hoar, T. J. (1997). El Niño and climate change. *Geophysical Research Letters*, 24(23), 3057–3060.

Tyson, P. D., & Preston-Whyte, R. A. (2000). The Weather and Climate of Southern Africa (2nd ed.). Oxford University Press Southern Africa, Cape Town.

University Corporation for Atmospheric Research (UCAR). (2024). Niño SST Indices (Niño 1+2, 3, 3.4, 4; ONI and TNI). Climate Data Guide. Retrieved from https://climatedataguide.ucar.edu/climate-data/nino-sst-indices-nino-12-3-34-4-oni-and-tni

United Nations Office for Disaster Risk Reduction (UNDRR). (2024, September 11). Horn of Africa floods and drought, 2020–2023 – Forensic analysis. UNDRR Case Study. Retrieved from https://www.undrr.org/resource/horn-africa-floods-and-drought-2020-2023-forensic-analysis

United Nations Office for the Coordination of Humanitarian Affairs (OCHA). (2023, December 14). Eastern Africa: El Niño impact snapshot (December 2023). OCHA Report. Retrieved from https://www.unocha.org/publications/report/somalia/eastern-africa-el-nino-impact-snapshot-december-2023

Vecchi, G. A., & Harrison, D. E. (2000). Tropical Pacific sea surface temperature anomalies, El Niño, and equatorial westerly wind events. Journal of Climate, 13(11), 1814–1830.

Vecchi, G. A., & Harrison, D. E. (2006). The termination of the 1997–98 El Niño. Part I: Mechanisms of oceanic change. Journal of Climate, 19(12), 2633–2646.

Vecchi, G. A., & Soden, B. J. (2007). Effect of remote sea surface temperature change on tropical cyclone potential intensity. Nature, 450(7172), 1066–1070.

Villalobos, H., Buenfil-Ávila, A., Ortega-García, S., Jakes-Cota, U., Moncayo-Estrada, R., & Reygondeau, G. (2024). Reanalysis of sea surface anomaly events in the Eastern Pacific Ocean in the first two decades of the 21st century. SSRN Working Paper.

Wang, C., Deser, C., Yu, J.-Y., DiNezio, P., & Clement, A. (2017). El Niño and Southern Oscillation (ENSO): A review. In P. W. Glynn, D. P. Manzello, & I. C. Enochs (Eds.), Coral Reefs of the Eastern Tropical Pacific (Coral Reefs of the World, Vol. 8, pp. 85–106). Springer.

Ward, P. J., Jongman, B., Kummu, M., Dettinger, M. D., & Winsemius, H. C. (2014). Strong influence of El Niño Southern Oscillation on flood risk around the world. Proceedings of the National Academy of Sciences (PNAS), 111(44), 15659–15664.

Yeh, S.-W., Kug, J.-S., Dewitte, B., Kwon, M.-H., Kirtman, B. P., & Jin, F.-F. (2018). ENSO atmospheric teleconnections and their response to greenhouse gas forcing. Reviews of Geophysics, 56(1), 185–206.

Yu, J.-Y., & Kao, H.-Y. (2007). Decadal changes of ENSO persistence barrier in SST and ocean heat content indices: 1958–2001. Journal of Geophysical Research: Atmospheres, 112(D13), D13106. https://doi.org/10.1029/2006JD007654